

A comparison of glacial and land-use controls on erosion in the northeastern United States

Author: Elisabeth M. Ames

Persistent link: <http://hdl.handle.net/2345/bc-ir:108252>

This work is posted on [eScholarship@BC](#),
Boston College University Libraries.

Boston College Electronic Thesis or Dissertation, 2018

Copyright is held by the author, with all rights reserved, unless otherwise noted.

A COMPARISON OF GLACIAL AND LAND-USE CONTROLS ON EROSION IN THE NORTHEASTERN UNITED STATES

Elisabeth M. Ames

A thesis
Submitted to the Faculty of
the department of Earth and Environmental Sciences
in partial fulfillment
of the requirements for the degree of
Master of Science

Boston College
Morrissey College of Arts and Sciences
Graduate School

May 2018

A COMPARISON OF GLACIAL AND LAND-USE CONTROLS ON EROSION IN THE NORTHEASTERN UNITED STATES

Elisabeth M. Ames

Advisor: Noah P. Snyder, Ph.D.

Global studies assert that anthropogenic activity now leads to disproportionately higher rates of landscape change compared with background geomorphic processes. This study explores the relative influence of anthropogenic, glacial, and geologic processes on erosion rates (E) in the northeastern United States (NEUS) by analyzing published erosion and sedimentation data across multiple methods and timescales. I compile erosion rates and sediment yields from records of stream gauging, reservoir sedimentation, lake sedimentation, cosmogenic nuclides in stream sediment, and thermochronology. These data serve as a comparison point for quantified volumes of sediment deposited in valley bottoms as a result of European settlement in the NEUS, where glacial history may influence the availability of erodible sediment and, as a result, the relative magnitude of deposited sediment. I hypothesize that E in the formerly glaciated region will be lower than unglaciated E over last century (stream gauging and reservoir sedimentation) timescales due to the erosive power of continental glaciation and resultant thin upland soils, and that there will be an increase in E evident over the last century as a result of human influence. 499 sites with location data were compiled across the NEUS, converted to erosion rate (mm/yr) and sediment yield (Y_s ; $t\ km^{-2}\ yr^{-1}$), and analyzed using statistical z-tests to determine whether the population means are significantly different. Mean E from all record types across both the glaciated and unglaciated NEUS exhibits a range smaller than one order of magnitude (0.012-0.055 mm/yr), much less variable than order-of-magnitude differences reported by other researchers comparing modern and geologic erosion, both regionally and globally. Last century

timescales exhibit higher E in the unglaciated region than the glaciated region, but only reservoir sedimentation shows a significant difference in E between regions (0.012 vs. 0.055 mm/yr; glaciated and unglaciated, respectively); stream gauging E did not exhibit a significant regional difference, likely due to the large basin sizes, short measurement timescales, and disproportionate spatial distribution of the measurements. E does not increase from geologic to last century timescales: late Quaternary (lake sedimentation and cosmogenic nuclide) records consistently yield lowest E , with geologic (thermochronology) records showing the highest E in both regions, perhaps indicating the relative importance of E over timescales during which major orogenies were occurring in the NEUS. The similarities in mean E and large range of the distributions of all timescales, however, point to the relative stability of E over time in the NEUS.

ACKNOWLEDGEMENTS

This research was supported by NSF Grant 1451562. I am indebted to the Boston College Earth and Environmental Sciences department for support in the form of teaching assistantships, as well as funding for travel to conferences over my time at BC. I am grateful to all the professors I had during my time here – your dedication to teaching is apparent and much appreciated.

Dorothy and Bob – thank you for your continued input and seemingly unlimited knowledge, as well as the opportunity to tag along on some really fantastic field trips.

Aakash Ahamed, Tim Cook, and Ryan McKeon – thank you for sharing your data as well as your input on this research. Joanna Reuter, thank you for sending your copious and well-kept data on cosmogenic nuclide concentrations in the Susquehanna River Basin.

Noah – thank you so much for your advocacy and support. Your guidance means a lot to me, but thank you also for fostering the trust and independence I needed to strike out on my own.

Corinne and Paul – thank you for serving on my committee. Your questions and input allowed me to expand and improve this research considerably.

Fellow grad students – thank you for your collaboration, openness, and selfless friendship. The community I had here was truly special, and I wouldn't have gotten through half my classes without your knowledge and willingness to share it.

Sam and Kate – the best milldamsels a girl could ask for. Kate, thank you for being the “older sister” and reminiscing about the Midwest with me. Sam, thank you for being a great roommate, trusted chauffeur, and patient friend.

Jon – your patience and kindness are unparalleled, and I am truly lucky you're by my side. Thanks also for all the bread.

Friends and family – thank you for your support throughout this process. You are all wonderful listeners, even if you were secretly tired of hearing me talk about erosion.

TABLE of CONTENTS

ACKNOWLEDGEMENTS	i
LIST of FIGURES	iv
LIST of TABLES	vi
1. INTRODUCTION	1
1.1 Study objectives	2
1.2 Previous work and study motivation	3
1.2.1 Global estimates of erosion and soil production	3
1.2.2 Controls on erosion rate (E) and sediment yield (Y_s)	5
1.2.3 Erosion in eastern North America	7
1.3 Hypotheses	9
2. METHODS	11
2.1 Records of erosion and sedimentation	11
2.1.1 Stream gauging	13
2.1.2 Lake and reservoir sedimentation	14
2.1.3 Cosmogenic nuclides	16
2.1.4 Thermochronology	17
2.2 Calculations and statistical analysis	19
2.2.1 Calculating erosion (E) and sediment yield (Y_s)	19
2.2.2 Two-sample z-tests	21
2.3 Assumptions in rate comparisons	21
3. RESULTS	23
3.1 Data finalization and E , Y_s statistics	23
3.2 Comparing E in the glaciated and unglaciated NEUS	25
3.2.1 Stream gauging and reservoir sedimentation (last century E)	25
3.2.2 Lake sedimentation and cosmogenic nuclides (late Quaternary E)	29
3.2.3 Thermochronology (geologic E)	31

3.3 Comparing E across erosional timescales	33
3.3.1 Glaciated region	33
3.3.2 Unglaciated region	35
3.3.3 Combined	36
3.4 Drainage basin area (A_B) as a control on E	38
4. DISCUSSION	40
4.1 Comparing NEUS E with global E	40
4.2 Comparing E in the glaciated and unglaciated NEUS	41
4.2.1 Last century E : Stream gauging and reservoir sedimentation	41
4.2.2 Late quaternary E : Lake sedimentation and cosmogenic nuclides	44
4.2.3 Geologic E : Thermochronology	44
4.3 Comparing E across erosional timescales	46
5. SUMMARY AND CONCLUSIONS	49
REFERENCES	51
APPENDIX 1: Y_s , E , location, drainage area, and timescale data for all points	57

LIST of FIGURES

Figure 1.1 Extent of Laurentide glaciation in the NEUS	3
Figure 2.1 Conceptual representation of watersheds with representative locations at which E may be measured	11
Figure 3.1 Spatial distribution of erosion rates by record type	24
Figure 3.2 Spatial distribution of last century E	26
Figure 3.3 Log-scale histograms of stream gauging E by region. Z-test results: $h_1 = 0$; $h_2 = 1$	27
Figure 3.4 Log-scale histograms of reservoir sedimentation E by region. Z-test results: $h_1 = 1$; $h_2 = 1$	27
Figure 3.5 Log-scale histograms of last century E (stream gauging and reservoir sedimentation combined) by region. Z-test results: $h_1 = 1$; $h_2 = 1$	28
Figure 3.6 Spatial distribution of late Quaternary E (lake sedimentation and cosmogenic nuclides)	30
Figure 3.7 Log-scale histograms of E for lake sedimentation (A) and cosmogenic nuclides (B). Z-test results: $h_1 = 0$; $h_2 = 0$	30
Figure 3.8 Spatial distribution of geologic E (thermochronology)	31
Figure 3.9 Log-scale histograms of geologic E (thermochronology) by region. Z-test results: $h_1 = 0$; $h_2 = 0$	32
Figure 3.10 Log-scale histograms of E by record type (shortest timescale to longest) for the glaciated region	34
Figure 3.11 Log-scale histograms of E by record type (shortest timescale to longest) for the unglaciated region	35
Figure 3.12 E versus T for all points, by record type. Cosmogenic nuclide data fall along a straight line because attenuation depth of ^{10}Be (165 cm below the surface; Reuter, 2005) was divided by erosion rate in order to obtain the timescale over which erosion occurred	37
Figure 3.13 Comparison of E by record type. Boxes represent the ranges of erosion rates and timescales, with timescale of measurement represented by their width	37

Figure 3.14 Logarithmic plots of E versus drainage basin area for all points with available area data (excluding thermochronology). A: Stream gauging; B: Reservoir sedimentation; C: Lake sedimentation; D: Cosmogenic nuclides; E: All points 39

LIST of TABLES

Table 1.1 Average global erosion and soil production rates from previously published studies ..	5
Table 2.1 Types of records compiled in this study, their original reported quantities, and timescales over which they are measured	12
Table 2.2 Overview of methods for calculations; measurements and their base units. Actual units of measurements vary by source and may require conversion prior to calculation	20
Table 3.1 Statistics for each record type: E (erosion rate; mm/yr), Y_S (sediment yield; t km ⁻² yr ⁻¹) and T (averaging timescale; years). Converted mean E (calculated with logarithmic data and converted to normal space) is mean E referred to in the text, and used in all statistical analysis	24
Table 3.2 H and p -values for z -tests between spatially compared record types (h_1 and p_1 indicate the likelihood that the glaciated population can be described by the mean of the unglaciated population; h_2 and p_2 indicate the opposite). H values of 1 indicate that the null hypothesis – that the mean of one population can describe the other – is not supported, with $p \leq 0.05$, and the populations can be considered statistically different	28
Table 3.3 H and p -values for z -tests between record types in the glaciated region (h_1 and p_1 indicate the likelihood that the first listed population can be described by the mean of the second population; h_2 and p_2 indicate the opposite). H values of 1 indicate that the null hypothesis – that the mean of one population can describe the other – is not supported, with $p \leq 0.05$	34
Table 3.4 H and p -values for z -tests between record types in the unglaciated region. H_1 and p_1 indicate the likelihood that the first listed population can be described by the mean of the second population; h_2 and p_2 indicate the opposite. H values of 1 indicate that the null hypothesis – that the mean of one population can describe the other – is not supported, with $p \leq 0.05$	36

1. INTRODUCTION

Globally, humans are moving increasing volumes of rock and soil around the landscape, arguably becoming the most powerful geomorphic driver currently affecting the surface of the Earth (Hooke, 2000; Wilkinson, 2005; Wilkinson and McElroy, 2007). Modern erosion largely occurs via deforestation (e.g., Bormann et al., 1974), construction (e.g., Wolman and Schick, 1967), and agriculture (e.g., Montgomery, 2007). Quantifying the effects of anthropogenic erosion is important in making land management decisions (Allmendinger et al., 2007), balancing large scale sediment budgets (e.g., Trimble, 1981), and for the overall understanding of how the presence of humans has modified the surface of the Earth. Many modern studies have shown a significant increase in anthropogenic erosion rate compared with geologic rates (e.g., Clapp et al., 2000; Schaller et al., 2001), with some modern rates exceeding background erosion rates by an order of magnitude or more (e.g., Walling, 1999; Hewawasam et al., 2003; Reuter, 2005; Montgomery, 2007; Reusser et al., 2015). Erosion estimates given by Wilkinson (2005) give natural rates of denudation around 0.02 mm/yr, whereas the global movement of soil via construction and agriculture is presently 0.57 mm/yr (Hooke, 2000), over ten times the background erosion rate.

The climatic history of a landscape may influence erosional processes. Continental glaciation is a significant erosive force, with late glacial erosion rates exceeding present day denudation by an order of magnitude or more (Syvitski and Milliman, 2007). An estimated 120 meters of physical erosion induced by the Laurentide Ice Sheet since the beginning of glaciation in North America was given by Bell and Laine (1985), through the processes of the stripping of regolith and plucking by ice sheets, fluvial erosion of glacial drift, and the delivery of sediment to oceans via interglacial, proglacial, and meltwater streams. The stripping of sediment by ice

sheets leaves behind landscapes with lower post-glacial sediment yields (e.g., Gordon, 1979) due to thin upland soils and the addition of terrestrial accommodation space in the form of lakes and wetlands (Snyder et al., 2013).

1.1 Study objectives

This study compiles and analyzes published values of erosion and sedimentation in the northeastern United States (NEUS), serving as a basis with which to consider whether anthropogenic activity and glacial history have had an effect on sediment movement in the glaciated and unglaciated regions of the study area (Figure 1.1). I assemble records of denudation from thermochronology of mountain ranges; erosion from concentrations of cosmogenic nuclides in river sediment; volumes of sediment stored in lakes and reservoirs; and suspended sediment concentrations from stream gauging, and estimate from them watershed-scale sediment yield (Y_s) and erosion rate (E). I then use these compiled records to compare rates of sediment movement between both glaciated and unglaciated portions of the NEUS, as well as to quantify changes in erosion and sediment delivery on geologic to modern timescales.

Sediment yield (Y_s), or the mass of sediment eroded per basin area over time (Griffiths et al., 2006), can be utilized to quantify the rate of erosion in the upstream portion of the watershed in which it is measured (Evans et al., 2000). Similarly, basin-wide erosion rates (E), or how much rock and soil is eroded over time, can be used to estimate Y_s . Both measurement types quantify the removal of sediment from a drainage basin and may be used interchangeably, under assumptions detailed in section 2.2. I will use the term “erosion” throughout this thesis to refer to both quantities; the relationships presented are equally applicable when defined in terms of Y_s .

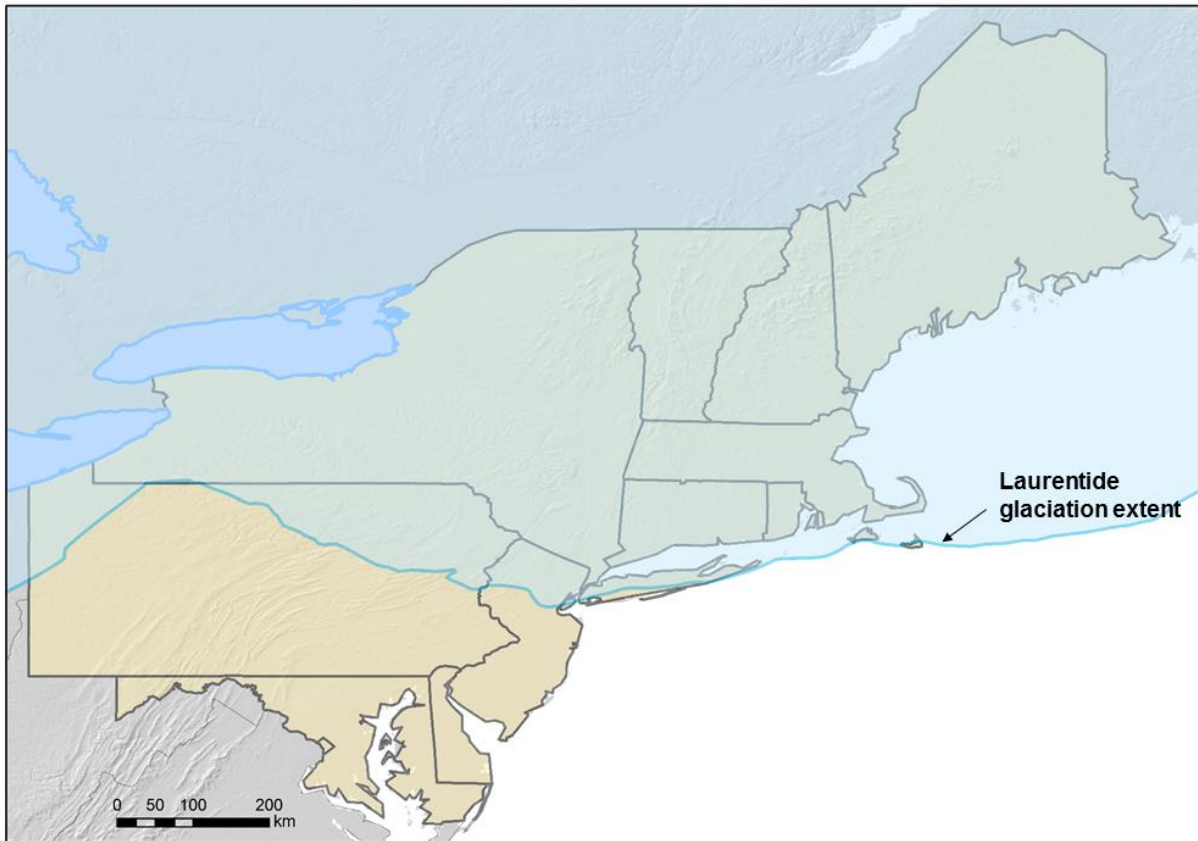


Figure 1.1 Extent of Laurentide glaciation in the NEUS.

1.2 Previous work and study motivation

1.2.1 Global estimates of erosion and soil production

Global compilations of denudation rates overwhelmingly cite an increase in erosion from geologic to human timescales. Geologic E , measured over timescales of roughly 10^4 to 10^7 year timescales and derived from thermochronology, volumes of sedimentary rock, and concentrations of cosmogenic nuclides in stream sediment, ranges from 0.016 to 0.226 mm/yr (Table 1.1). Wilkinson (2005) and Wilkinson and McElroy (2007) used volumes of Phanerozoic offshore sedimentary rock to reconstruct epoch-long denudation rates more than an order of magnitude lower than 20th century mean river-derived sediment loads, which they interpret as a result of erosion associated with modern construction and agriculture.

Background soil production rates fall within the range of geologic E , with estimates from 0.036 to 0.083 mm/yr (Table 1.1). Cropland E , however, generally shows a tenfold increase over background erosion rates, with estimates between 0.4 and 4 mm/yr. Compilations of global fluvial sediment flux encompassing ca. the last 100 years are less common, but bridge the gap between geologic and agricultural denudation rates with a wide range of 0.069 to 0.751 mm/yr (Table 1.1). In general, lowland, cratonic landscapes yield the lowest geologic erosion rates, while steep, tectonically active landscapes give the highest (Montgomery, 2007).

A number of studies have compared erosion and sedimentation rates across multiple spatial and time scales. Koppes and Montgomery (2009) studied the relative erosive impact of rivers and glaciers over modern to orogenic timescales, finding that tectonic activity tends to exert the most control over erosion in thousand-year timescales and longer, with modern agricultural E on par with alpine E in the most tectonically active mountain belts. Montgomery (2007) compiled global rates of agricultural E from conventionally plowed fields and found that on average, they are 1 to 2 orders of magnitude greater than soil production rates and long-term geological E , derived largely from thermochronologic and cosmogenic nuclide studies.

In contrast, Kirchner et al. (2001) found that geologic E measured with apatite fission track thermochronology and cosmogenic ^{10}Be in small Idaho mountain catchments exceeded modern stream sediment fluxes, which they interpret as a result of the infrequent recurrence of large floods over the relatively short modern time interval, therefore delivering sediment only sporadically. Covault et al. (2013) compared global studies of E derived from cosmogenic nuclides (majority ^{10}Be) and stream gauging in order to assess spatial and temporal patterns associated with landscape evolution. They plotted cosmogenic nuclide-derived sediment loads against stream gauge loads at locations where the two basins were no more than 500 km apart. At

about two thirds of measured locations, cosmogenic sediment loads were greater than historic loads, likely as a result of the longer-term recurrence of large sediment transport events; however, at 80% of locations, the two measurements were within an order of magnitude of one another, which they attribute to the buffering capacity of large floodplains.

Table 1.1 Average global erosion and soil production rates from previously published studies.

Source	Erosion (mm/yr)	Method notes
<i>Geologic erosion</i>		
Montgomery and Brandon, 2002	0.017	Low-temperature thermochronometry
Wilkinson, 2005	0.024	
Wilkinson and McElroy, 2007	0.016	
Montgomery, 2007	0.036	
Portenga and Bierman, 2011	0.218	¹⁰ Be catchment denudation
Covault et al., 2013	0.226	Cosmogenic catchment denudation
<i>Soil production</i>		
Wakatsuki and Rasyidin, 1992	0.058	
Troeh et al., 1999	0.083	
Montgomery, 2007	0.036	
<i>Agricultural erosion</i>		
USDA, 1988	0.400	
Pimentel et al., 1995	0.680	Cropland tillage (developed)
Hooke, 2000	0.570	
Pimentel and Skidmore, 2004	1.40	Cropland tillage (undeveloped)
Wilkinson and McElroy, 2007	0.885	Cropland denudation, U.S. (USLE)
Montgomery, 2007	3.939	
<i>Fluvial sediment flux</i>		
Summerfield and Hulton, 1994	0.069	
Milliman and Farnsworth, 2011	0.110	
Covault et al., 2013	0.751	

1.2.2 Controls on erosion rate (E) and sediment yield (Y_s)

A number of factors may affect the rate and quantity of downstream sediment delivery, including (but not limited to) drainage basin morphology (e.g., basin size, relief, and slope; Milliman and Syvitski, 1992; Ahnert, 1970 and Summerfield and Hulton, 1994; and

Montgomery and Brandon, 2002, respectively); bedrock geology; climate (precipitation and runoff; e.g., Langbein and Schumm, 1958; Tardy et al., 1989); vegetation cover; and anthropogenic activity.

Most basins evolve to a steady state between tectonic uplift and erosion. Erosion rates are tied strongly to high gradients, so rapidly uplifting basins exhibit steeper slopes. For this reason, morphological characteristics of drainage basins, such as slope, relief, and elevation, have classically been used as a proxy for the tectonic activity of a watershed (Covault et al., 2013). Relief and slope fundamentally quantify watershed gradient. Studies on local relief, or the difference between the highest and lowest point in a watershed, suggest relief has significant impact on sediment delivery, with Ahnert (1970) reporting a linear relationship between relief and E , and Summerfield and Hulton (1994) finding that 60% of variation in the denudation of global drainage basins could be explained by basin relief ratio and runoff. In low-slope watersheds in the Olympic Mountain range, Montgomery and Brandon (2002) found a linear relationship between slope and E ; in steeper watersheds (slope greater than 25°), a power law relationship exists. In lower-gradient, tectonically inactive regions like the NEUS, the relationship between slope and E can be less clear (e.g. Ahamed, 2014).

Although sediment loads generally increase with drainage area (A_B), given that larger catchments will have more surface area from which to source sediment, sediment yields (Y_s , in which load is normalized to A_B) tend to decrease with increasing basin size. Milliman and Syvitski (1992) found an inverse relationship between drainage area and Y_s upon analyzing global rivers, attributing this result to the ability for larger watersheds to store more sediment upstream and on floodplains. Ahamed (2014) calculated Y_s from reservoirs in the states east of

the Mississippi River and found a weak inverse power law relationship between Y_s and A_B , also attributable to the greater storage capacity (e.g., in terraces and lakes) of larger basins.

Much work has been done attempting to deconvolve the movement of sediment from these controls, yet no universal relationship has been discovered. This is because the sediment flux within a drainage basin is a function of the integrated tectonic, geomorphic, and climatic processes within it (Hovius and Leeder, 1998), and local variability controls the complicated interaction between these processes. In general, however, Syvitski and Milliman (2007) found that geological factors (basin relief, area, lithology, and glacial erosion) account for approximately two thirds of the variation in global sediment loads, whereas climatic and anthropogenic activity explains the additional third.

1.2.3 Erosion in eastern North America

Studies assessing spatial and temporal variations in E in the eastern part of North America are prevalent. Conrad (2000) evaluated reported sediment yields (Y_s) in the eastern provinces of Canada and the eastern coastal United States using data from 193 gauging stations, finding a general inverse relationship between latitude and Y_s . She attributes this relationship to a number of potential factors: population centers are smaller farther north; gauging stations are farther from major urban centers in Canada than the U.S.; surface erosion is reduced at higher latitudes due to frozen and snow-covered surfaces; and there is a lack of thick, erodible soil above the glacial limit, where surfaces are characterized by thin soil horizons and bedrock. Ahamed (2014) conducted analysis on controls contributing to reservoir sedimentation rates in study watersheds east of the Mississippi River, finding that glacial history, mean annual temperature, percentage of impervious surface area, and sedimentation timescale show the most significant relationships with calculated Y_s . Land-use changes through time are also argued to

have a significant effect on E ; Meade (1969) posits that Y_s in the eastern United States were four to five times lower prior to European settlement. He estimated a tenfold increase in Y_s due to the post-settlement conversion of forests to cropland, and cites the continuing influence of coal mining, urbanization, and construction on additional sediment loading in modern streams.

Exaggerated rates of modern erosion in the Mid Atlantic states have captured the interest of researchers since the 1960s. Many cite the effects of human activity on sediment loss, whether related to European settlement and subsequent deforestation for agriculture (Costa, 1975; Brush, 1984) or continued high-impact construction of urban areas into the present day (Wolman and Schick, 1967). Walter and Merritts (2008) proposed that the coincidence of land clearing by European settlers with the construction of milldams on streams in the Mid Atlantic region led to the accumulation of large volumes of sediment in millponds. This legacy sediment, deposited in the last three to four centuries, has the capacity to persist for hundreds of years. Subsequent breaching of the dams, either by removal or natural deterioration, has led to a lowering of base level, incision through the deposited sediment, and sediment delivery downstream, with implications for watershed management and beyond. A handful of studies have also investigated pre-settlement E in the Mid Atlantic and farther south in the Appalachians (e.g., Reuter, 2005; Reusser et al., 2015). The aforementioned studies found that modern Y_s values are roughly one order of magnitude greater than those derived from cosmogenic nuclide concentrations in river sediment.

Meade (1982) found a poor relationship between sediment concentration and streamflow in New England, inferring the influence of intense glaciation on the resultant low sediment supply, whereas the rest of the Atlantic Coastal Plain exhibited high sediment concentrations with streamflow. Denudation rates are low in central New England because many streams flow

over stable, erosion-resistant glacial materials (Gordon, 1979), and the combination of dense vegetation with poor surface drainage locally produces relatively low Y_s (Anderson and George, 1966). At the same time, milldam density, and therefore the potential to trap large quantities of sediment (Walter and Merritts, 2008) is similar between the glaciated and unglaciated NEUS. This similarity, contrasted with the dissimilarity of the regions' glacial history, and therefore availability of erodible sediment, provides a unique angle from which to study erosion in the NEUS.

The overarching purpose of this study is to serve as a comparison point for quantified volumes of legacy sediment associated with European settlement in valley bottoms of the NEUS, which bridge the gap between geological to late Quaternary erosion rates and erosion rates encompassing roughly the last century. As a result, the relative influence of geologic, climate-driven, and anthropogenic processes on landscape change in the NEUS can be determined. This study also seeks to address whether the assertion that globally, the influence of anthropogenic activity on the movement of rock and soil from hillslopes to valley bottoms is now greater than that of geologic processes (Wilkinson and McElroy, 2007), holds true on a regional scale.

1.3 Hypotheses

This thesis aims to address the following question: How do rates of erosion and sedimentation vary by region and by timescale in the northeastern United States? Two hypotheses are proposed.

1. *Spatial hypothesis*: Erosion rates (E) and sediment yields (Y_s) are lower in the glaciated region than the unglaciated region over last century (stream gauging; reservoir sedimentation) timescales.

2. *Temporal hypothesis*: Geologic (10^5 to 10^7 year timescales) and late Quaternary (10^3 to 10^5 year timescales) E and Y_s , given by thermochronology, cosmogenic nuclide, and lake sedimentation studies, are lower than last century rates across both the glaciated and unglaciated regions.

2. METHODS

The sediment budget of a drainage basin can be explained as the sediment flux into the basin (i.e. weathering and soil production) minus the sediment flux out of the basin (i.e. Y_s), which is equal to the change in storage within the basin (Figure 2.1). Measuring the mass of sediment stored within a basin (in terraces, lakes, or wetlands, for example) can give an estimate of sediment delivery, as well as constrain E up-basin (Bierman and Montgomery, 2014); lake and reservoir sedimentation studies are extensive in the NEUS. Rates of erosion, sediment storage, and sediment yield will all be compiled for my thesis research in an attempt to quantify basin-averaged erosion.

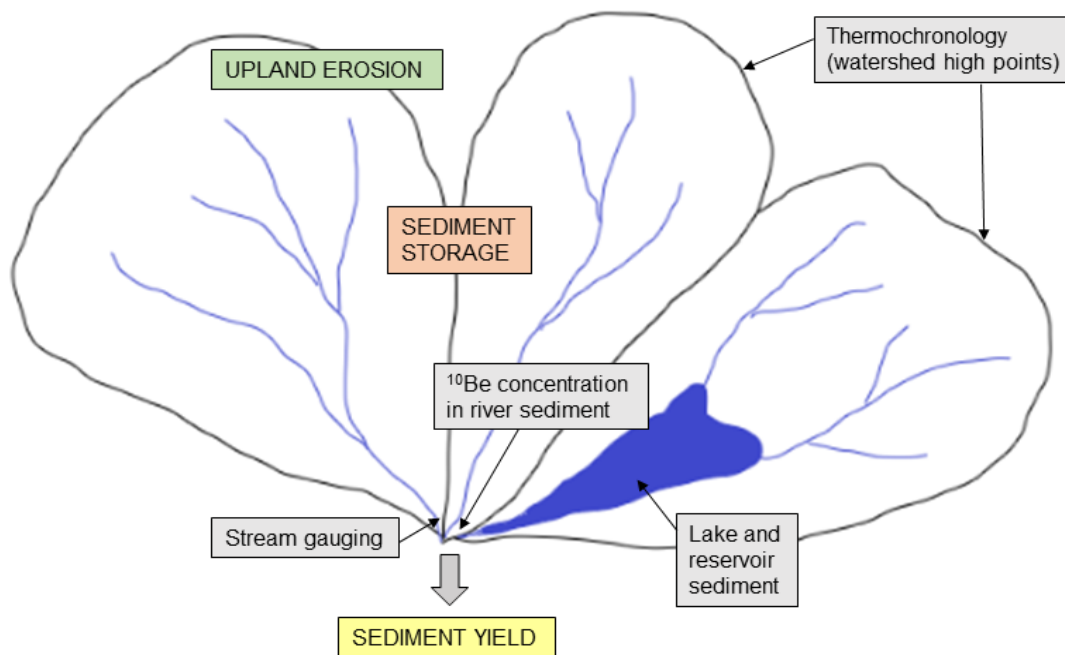


Figure 2.1 Conceptual representation of watersheds with representative locations at which E may be measured.

2.1 Records of erosion and sedimentation

A number of records are useful in determining rates, volumes, and yields of sediment stored and removed in watersheds across various regions and timescales. Estimates of the

volume of sediment eroded, which can then be converted into rates and/or yields, can be made by measuring the amount of sediment stored in a lake or reservoir or by the gauging of sediment flux out of a watershed (Burbank and Anderson, 2012). Indirect, modeled methods, such as fission-track thermochronology and ^{10}Be concentrations in individual mineral grains, can also give inferred E . I compile inferred erosion and sedimentation rates from published records of stream gauging, lake and reservoir sediment cores, cosmogenic nuclide concentrations in stream sediment, and thermochronology (Table 2.1). The units in which these measurements were reported in the original sources were converted to Y_s and E as needed, as detailed in section 2.2.1.

Geographic coordinates were available for many of the measurements, and were recorded as such. Gauging stations without coordinates in their original sources were often searchable on the USGS web site; I obtained location information for the majority (those with incomplete or duplicate names were not used, e.g. if there were two stations on the same river and the correct one was ambiguous). Often, thermochronologic data were presented in map form without coordinates listed; in these cases, I used Google Earth to pinpoint the locations of the sample sites within about 10 km of their actual position, and transcribed their coordinates.

Measurements without viable location data were not used in the final study.

Table 2.1 Types of records compiled in this study, their original reported quantities, and timescales over which they are measured.

Measurement record	Erosion or sedimentation	Reported in	Timescale (years)
Stream gauging	Erosion	Mass/Area/Time	$10^0 - 10^1$
Reservoir cores	Sedimentation	Length/Time	$10^1 - 10^2$
Lake cores	Sedimentation	Length/Time	$10^2 - 10^4$
Cosmogenic nuclides	Erosion	Length/Time	$10^3 - 10^5$
Thermochronology	Erosion	Length/Time	10^5 and longer

2.1.1 Stream gauging

Stream gauging of Y_s measured at the outlet of a basin can provide information on rates of soil loss in the upstream watershed over annual to decadal timescales (Walling, 1994). Fluvial suspended sediment concentration may be measured directly by gauging station turbidity sensors that take frequent measurements. Many times, however, sediment concentration samples are taken manually and used in conjunction with stream flows to construct a sediment delivery rating curve, which is then used to estimate sediment flux (Q_s), the mass of dissolved and particulate matter of a river, at times when in situ sediment sampling does not occur. Stream gauging Y_s is thought to be sensitive to, and therefore good recorders of, anthropogenic disturbances like deforestation, mining, and land use change.

The majority of Q_s data from stream gauging are from USGS reports from the NEUS over approximately the last 50 years. Many of these studies concern streams in and around the Chesapeake Bay region, and fewer have been done in New England. The reports used all calculated suspended sediment flux only; bed load and dissolved loads are not included in the estimates. Bed load is commonly assumed to be approximately 10% of the suspended load; dissolved load varies considerably based on drainage basin climate and lithology (Judson and Ritter, 1964), and is generally higher in warm, wet and carbonate-dominated landscapes.

Stream gauge records may underrepresent the amount of erosion occurring in a basin, as not all sediment eroded within it will exit as stream load; some will be stored within the catchment, in lakes and wetlands, on floodplains, and, behind dams. Trimble (1977) found that ten large (2,650 to 19,400 km²) river basins in the United States give sediment delivery ratios (SDRs) of about 6%; larger basins especially may experience low SDR, as more sediment is

stored as alluvium within the basin. Smaller basins should give better estimates of sediment delivery, as there will be less space for sediment to accumulate.

Stream gauge data are usually available only over the span of several years, which may not be representative of sediment transport over longer intervals (Meade, 1969; Kirchner et al., 2001); conversely, unrepresentative Y_s may be captured by stream gauging if an anomalously large flood occurs during the period of record. Therefore, longer gauging records should be used wherever possible. Milliman and Farnsworth (2011) provide an excellent summary of the many potential problems with stream gauging records, including inconsistencies with measurement, uneven geographic distribution of gauging stations, and the length of record. Despite the errors associated with Y_s estimates from stream gauging, the method is widespread in use and therefore one of the most useful for consistently estimating modern sediment yields.

2.1.2 Lake and reservoir sedimentation

Rates of sedimentation in a lake or reservoir can be determined by extrapolating from sediment cores taken over the depositional area, assuming either consistent or variable layer thickness (Snyder et al., 2004). In reservoirs with steady sedimentation, repeat bathymetric surveys are often used to determine sediment thickness, which can be divided by the age of the reservoir to obtain a sedimentation rate; in lakes or reservoirs without pre-determined bathymetry, however, rates can be determined by locating and dating horizons within the sediment, using sediment cores (Morris and Fan, 1998). Modern sedimentation rates can be obtained by the dating of the anthropogenic radionuclide ^{137}Cs in sediment, a product of atomic bomb testing in the 1950s, or natural radionuclide ^{210}Pb (Edgington et al., 1991). Radiocarbon (^{14}C) dating of organic material can provide similar chronological control on lake sediments (MacDonald et al., 1991). The presence of indicator species of pollen may also constrain the

timing over which sediment is deposited (Davis, 1969). In this way, rates of lake and reservoir sedimentation can be measured over annual to millennial timescales.

Erosion rates in this study are compiled from Ahamed (2014) (reservoir sedimentation) and a database of existing lake sedimentation studies in New England compiled by Timothy Cook (personal communication). Ahamed (2014) used ResSed, a subset of the National Inventory of Dams, to calculate Y_s in available reservoirs in the eastern United States. The surveys were conducted by the United States Army Corps of Engineers via either measuring bathymetry or the collection of sediment cores. The reservoirs range in size, but contain data mostly from reservoirs $< 100 \text{ km}^2$. 95% of the surveys were conducted between 1930 and 1990. Y_s and E were quantified by Ahamed (2014) using a model developed in ArcGIS.

Cook (pers. comm.) compiled sedimentation rates from existing NEUS limnological studies, as well as lake and drainage basin characteristics, age control types (^{210}Pb , ^{137}Cs , pollen, ^{14}C), and water quality measurements, where applicable. I calculated E and Y_s using sedimentation rate ($Q_{s,lin}$), lake area (A_R), and drainage basin area (A_B) where possible, assuming constant layer thickness over the area of the lake (see section 2.2.1 for calculation details).

In lakes, sediment mixing (e.g., bioturbation) and down-core compaction may make sedimentation rates misleading or difficult to acquire. Trap efficiency, or the proportion of incoming sediment that is deposited in a lake or reservoir (Verstraeten and Poesen, 2000), is one of the largest sources of uncertainty in determining Y_s from sedimentation rate. In all likelihood, the lakes and reservoirs from which E is calculated do not impound all sediment transported through them. Ahamed (2014) corrected for the trapping effect of upstream dams in the ResSed database; however, no corrections were made for suspended sediment traveling through the dam

outlet. Therefore, in this case, erosion is treated as equal to sedimentation; these rates should be considered minima.

2.1.3 Cosmogenic nuclides

Concentrations of cosmogenic nuclides, typically ^{10}Be or ^{26}Al (^{10}Be in this study), in the quartz grains of river-bed sediment can be used to calculate an average rate of erosion over the entire upstream area of a basin (Granger et al., 1996; Bierman and Stieg, 1996). Cosmogenic nuclides are produced in situ by the collision of high-energy particles with atmospheric molecules, which produces a cascade of cosmic rays, some of which reach the surface of the Earth and adsorb to rocks and minerals near the surface (von Blanckenburg, 2005). Nuclides rapidly attenuate with depth, so only near-surface processes are recorded; thus, their concentrations are integrated over timescales in which 1-2 m of soil is eroded (Bierman and Nichols, 2004). Because nuclide production decreases with depth, their concentration in a sediment sample essentially gives a history of the exposure time of that sample on a surface: the higher the concentration, the slower the erosion rate (Granger and Schaller, 2014). The time scale over which ^{10}Be is useful is approximately 10^3 to 10^5 years, which can fill the gap between erosion due to land use changes and that due to tectonic processes.

Erosion rates derived from cosmogenic nuclides used in this study were obtained by Joanna Reuter, from her 2005 M.S. thesis (University of Vermont) addressing rates and patterns of erosion in the Susquehanna River basin in New York, Pennsylvania, and Maryland, using Bierman and Steig's (1996) erosion calculation model based on ^{10}Be concentrations in quartz. More cosmogenic work has been conducted in the southern Appalachians and on bedrock incision rates (e.g., Matmon et al., 2003; Hancock and Kirwan, 2007; Portenga, 2011; Duxbury, 2015), but studies focused on basin-scale erosion in the NEUS generally remain sparse.

Von Blanckenburg (2005) lists several of the key assumptions made when using ^{10}Be to calculate E . First, the rate of landscape denudation must be constant over time, and the basin must be at cosmogenic steady state (production of nuclides in sediment equal to transport of sediment out of the basin). One must also assume that all sediment that is eroded from the catchment is eventually transported by the river, and that long-term sediment storage is minimal; this method is also thought not to be useful in places where human-induced erosion is so severe that deeply shielded sediment has been exposed. Drainage basin size must be taken into account, because large basins will store more sediment; in smaller basins, however, hillslope erosional events may not be incorporated as effectively into the sediment record (Burbank and Anderson, 2012). It must also be assumed that all lithologies present in the catchment are comparable and erode at a uniform rate, and that the loss of ^{10}Be by dissolution is inconsequential (Bierman and Nichols, 2004). Late Pleistocene glaciation also poses a problem with regard to the assumption of steady state due to shielding of sediment from cosmic rays by glacial ice; for this reason, no current studies exist above the extent of glaciation in the NEUS.

2.1.4 Thermochronology

Thermochronology uses radioisotopic dating to determine the timing and rates of orogenic exhumation, among other geologic applications (Reiners, 2005). This method is useful across timescales of about 10^5 to 10^7 years. The cooling depth of a given mineral (often apatite, zircon, or sphene) can be calculated by dividing the closure temperature of that mineral by the geothermal gradient (often the “typical” cooling rate of 20-30 °C/km), given by

$$Z = \frac{c}{dT/dz}, \quad (1)$$

where z is the depth, c is the closure temperature, and dT/dz is the geothermal gradient.

Exhumation rate, a proxy for E , can be determined by dividing the cooling depth by the timing of cooling through the closure temperature, given by

$$exhumation = \frac{z}{a}, \quad (2)$$

where a is the time of cooling through the closure temperature, given by radiometric dating or fission tracks (Burbank and Anderson, 2012). Multiple cooling ages within a watershed give an estimation of the average rate of exhumation, which can then be converted to Y_s .

The records I have compiled use either U-Th/He or apatite fission-track (AFT) thermochronology to calculate exhumation rates. Both methods are based on the production of an isotope (U-Th/He) or radiation damage (AFT) via nuclear decay, and how long a given mineral can thermally retain their decay products (Reiners and Brandon, 2006). Exhumation rates are often reported, but when they are not, I calculate them using the components included in their respective studies, including assumed dT/dz , most often 20°C/km. The majority of records obtained from the NEUS are from studies conducted by Mary Roden-Tice and colleagues, as she has worked extensively throughout the region.

Erosion rates based on thermochronologic estimates of exhumation, however, may be uncertain due to a variety of factors. Inference of the geothermal gradient, which varies both spatially and temporally, may be inaccurate, especially as the geothermal gradient is not constant during geotherm steepening in periods of rapid erosion (e.g., Winslow et al., 1994). Upper crustal isotherms are also sensitive to variations in topography. Local geotherms are often poorly defined, so the assumption of $dT/dz = 20 - 30$ °C/km may over- or underestimate the cooling rate. The assumed closure temperature of a given mineral may also be misleading, as it is

actually a range of temperatures through which the mineral starts to lose its daughter product (Bierman and Montgomery, 2014).

2.2 Calculations and statistical analysis

2.2.1 Calculating erosion (E) and sediment yield (Y_s)

Measurements reported in the literature were converted to Y_s and E for the comparison of both types of data; the general conversion method using base units can be found in Table 2.2. An example conversion is described as follows: sedimentation rates collected from lake cores are most often reported in depth of sediment deposited per time, or $Q_{s,lin}$ (mm or cm yr⁻¹); in order to convert to a basin-wide erosion rate, one must first multiply by the area of the lake (A_R) to obtain volumetric sediment flux ($Q_{s,vol}$):

$$Q_{s,vol} = Q_{s,lin}A_R \cdot \quad (3)$$

This method assumes constant sedimentation throughout the lake; if several cores have been taken, a sedimentation rate may be extrapolated between them (Snyder et al., 2004). Mass sediment flux ($Q_{s,mass}$) is obtained by multiplying $Q_{s,vol}$ by sediment bulk density (ρ_s), an assumed value of 1200 kg/m³ for sediment in this study (Snyder et al., 2004):

$$Q_{s,mass} = Q_{s,vol}\rho_s \cdot \quad (4)$$

Y_s (mass per unit area per time) is obtained by dividing $Q_{s,vol}$ by the drainage basin area (A_B):

$$Y_s = \frac{Q_{s,mass}}{A_B} \cdot \quad (5)$$

Finally, E (length per time) is found by dividing Y_s by the density of eroded rock (ρ_R ; 2650 kg/m³ for quartz):

$$E = \frac{Y_s}{\rho_R} \cdot \quad (6)$$

Sedimentation in lake cores can then be compared with rates recorded using any other method mentioned above. The majority of other measurements are reported as either E or Y_s , which can easily be converted between by either multiplying or dividing by ρ_R . Stream gauging studies that report Q_s were divided by A_B as reported in the study, or by obtaining the area from the gauging station's respective USGS web page. Mean E and 1σ error referred to in the text and figures of this study were calculated on logarithmic-transformed data and converted to normal space.

Table 2.2 Overview of methods for calculations; measurements and their base units. Actual units of measurements vary by source and may require conversion prior to calculation.

Start	Units	Multiply by	Units	Output	Units
$Q_{S, lin}$	$m\ yr^{-1}$	A_R	m^2	$Q_{S, vol}$	$m^3\ yr^{-1}$
$Q_{S, vol}$	$m^3\ yr^{-1}$	ρ_S	$kg\ m^{-3}$	$Q_{S, mass}$	$kg\ yr^{-1}$
$Q_{S, mass}$	$kg\ yr^{-1}$	$1/A_B$	m^{-2}	Y_S	$kg\ m^{-2}\ yr^{-1}$
Y_S	$kg\ m^{-2}\ yr^{-1}$	$1/\rho_R$	$kg\ m^{-3}$	E	$m\ yr^{-1}$

ABBREVIATIONS

$Q_{S, lin}$	linear sedimentation rate
A_R	reservoir area
$Q_{S, vol}$	volumetric sedimentation rate
ρ_S	sediment bulk density
$Q_{S, mass}$	mass sedimentation rate
A_B	basin area
ρ_R	rock bulk density
Y_S	sediment yield
E	basin-averaged erosion rate

2.2.2 Two-sample z-tests

Once a sufficient sample of rates was compiled and converted to both E and Y_s (ideally, $n \geq 30$ for each type of record) (Appendix 1), statistical z-tests were used in order to test the null hypothesis that one data set can be described by the mean and standard deviation of another. Populations were log-transformed prior to testing, as ranges of E tend to span multiple orders of magnitude, and the data are log-normally distributed. Two z-tests were run for each pair of samples using Matlab: e.g., glaciated vs. unglaciated, then unglaciated vs. glaciated. The convention is such that h gives the z-test of (A, B, sigma), in which the data in sample A are hypothesized to come from a second distribution with mean B and 1σ error. $H = 0$ indicates that the null hypothesis (that the mean of A is B) cannot be rejected at the 5% significance level. Probability (p) values were computed for each z-test, with significant p-values (<0.05) indicating the high probability that the null hypothesis is not supported ($h = 1$). Log-axis histogram plots give a visual representation of the relative difference between regions and timescales, as well as the range in data. In this way, it can be determined whether there is a statistically significant dissimilarity between differing spatial or temporal data.

2.3 Assumptions in rate comparisons

A number of challenges arise from the comparison of erosion and sedimentation rates across the time and spatial scales examined in this study, including incomplete sediment delivery due to intrabasin storage, the magnitude and frequency of large floods with respect to sediment delivery, and erosional hiatuses in sedimentation over longer (late Quaternary and geologic) timescales. Care must be taken when interpreting rates from various records.

The sediment delivery ratio (SDR) refers to the amount of sediment leaving a basin via fluvial activity relative to the absolute amount of erosion occurring within the basin (Parsons et

al., 2006). The methods I use assume that $SDR = 1$, which may be questionable for stream gauging and cosmogenic nuclide records from large basins, where more floodplain storage occurs and a greater number of upstream lakes and reservoirs have the ability to trap eroded sediment.

Additionally, shorter-term estimates of Y_s are potentially uncertain due to the episodic nature of sediment transport (Summerfield and Hulton, 1994; Kirchner et al., 2001). Last century records (e.g., from stream gauging) should be used with caution, as they may under-represent the amount of transport occurring within a basin if they fail to capture large flood events; there may also be potential to overrepresent sediment transport if the record is short and happens to capture such a flood. Records of five or more years should be used whenever possible.

Obtaining rates from depositional systems (in this study, lake and reservoir sedimentation) yields another set of challenges. Last century sedimentation rates may either overrepresent large-scale sedimentation events or omit these events completely; late Quaternary sedimentation records, however, may include erosional episodes (unconformities) and subsequently under-preserve the stratigraphic record (Kirchner et al., 2001; Sadler and Jerolmack, 2014). Under-preservation should not be an issue in post-glacial New England lakes, however, where lake basins effectively trap sediment and have done so continuously since deglaciation. Additionally, the assumption of consistent layer thickness extrapolated over the area of a lake may either over- or under-represent the volume of existing sediment, depending on where cores were taken; sediment bulk density may also vary with sediment texture and the hydrologic conditions of the lake in question (e.g. Verstraeten and Poesen, 2001).

3. RESULTS

3.1 Data finalization and E , Y_s statistics

Six hundred twenty-three individual erosion (E), deposition, and sediment yield (Y_s) estimates were compiled throughout the NEUS, with 499 exhibiting viable location data (Figure 3.1; Appendix 1). All rates were converted both to a basin-averaged erosion rate (E ; mm/yr) and a sediment yield (Y_s ; t km⁻² yr⁻¹) as needed. These 499 sites were used in the following statistical analysis.

Stream gauging, reservoir sedimentation, and thermochronology estimates were compiled throughout both regions; lake sedimentation rates, however, have only been studied north of the glacial limit, as very few natural lakes exist to the south. Similarly, the only studies using cosmogenic nuclides in river sediment to determine E have been conducted south of the glacial limit, as the integrating timescales of ¹⁰Be span timescales of glaciation in the NEUS, potentially confounding results (Reuter, 2005).

The mean E for each of the record types are as follows: 0.017 mm/yr for stream gauging; 0.025 mm/yr for reservoir sedimentation; 0.012 mm/yr for lake sedimentation; 0.013 mm/yr for cosmogenic nuclides; and 0.031 mm/yr for thermochronology (Table 3.1). Stream gauging and reservoir sedimentation exhibit higher mean E in the unglaciated region (Table 3.1). Erosion rates for all record types span six orders of magnitude; however, their means are all within the same order of magnitude, with the exception of unglaciated reservoir sedimentation.

The timescales over which E is measured span nine orders of magnitude. Mean timescale (T , in years) of each record type is 7.2 years for stream gauging; 38.4 years for reservoir sedimentation; 8,170 years for lake sedimentation; 1.37×10^5 years for cosmogenic nuclides; and 1.41×10^8 years for thermochronology.

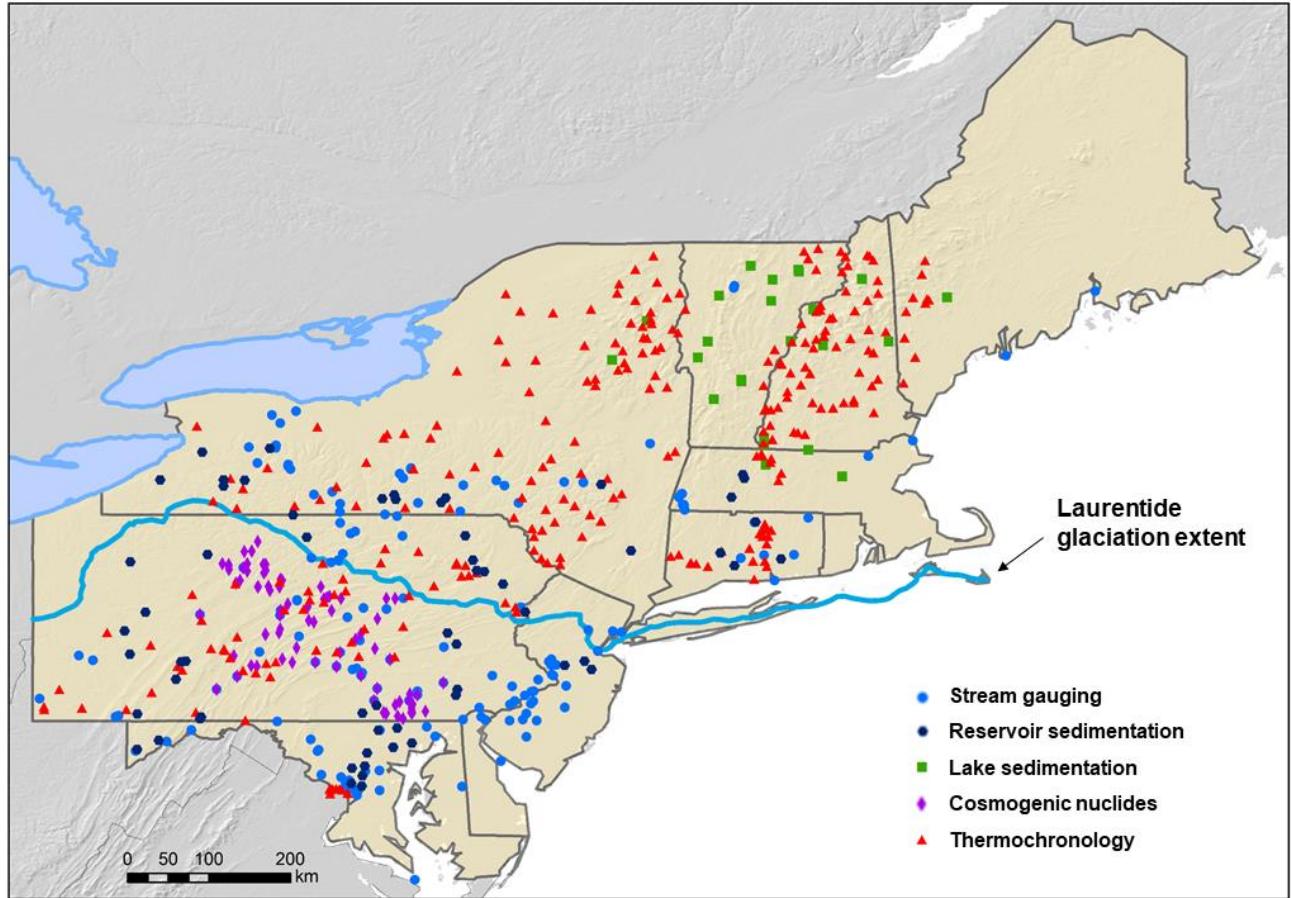


Figure 3.1 Spatial distribution of erosion rates by record type.

Table 3.1 Statistics for each record type: E (erosion rate; mm/yr), Y_s (sediment yield; $t\ km^{-2}\ yr^{-1}$) and T (averaging timescale; years). Converted mean E (calculated with logarithmic data and converted to normal space) is mean E referred to in the text, and used in all statistical analysis.

	Stream gauging		Reservoir sedimentation		Lake sedimentation	Cosmogenic nuclides	Thermochemistry	
	Glaciated	Unglaciated	Glaciated	Unglaciated	Glaciated	Unglaciated	Glaciated	Unglaciated
n	56	109	31	29	24	79	222	50
mean T	6	9.3	48.8	23.9	8170	137000	128×10^6	224×10^6
mean E	0.031 ± 0.054	0.068 ± 0.34	0.026 ± 0.049	0.12 ± 0.23	0.012 ± 0.016	0.009 ± 0.015	0.033 ± 0.012	0.034 ± 0.017
log-transformed E	-1.85 ± 0.57	-1.72 ± 0.56	-1.90 ± 0.47	-1.26 ± 0.53	-1.93 ± 0.34	-1.88 ± 0.23	-1.51 ± 0.17	-1.52 ± 0.18
converted mean E	0.014	0.019	0.012	0.055	0.012	0.013	0.031	0.030
error range (1σ)	0.004 - 0.051	0.005 - 0.070	0.004 - 0.037	0.016 - 0.186	0.005 - 0.026	0.008 - 0.022	0.021 - 0.046	0.020 - 0.046
mean Y_s	36.8	50.5	33.1	145	31.6	35.3	81.5	80.6
log-transformed Y_s	1.56 ± 0.57	1.70 ± 0.56	1.52 ± 0.47	2.16 ± 0.53	1.50 ± 0.35	1.54 ± 0.23	1.91 ± 0.17	1.91 ± 0.18
converted mean Y_s	36.8	50.5	33.1	145	31.6	35.3	81.5	80.6
error range (1σ)	9.98 - 136	13.8 - 185	11.2 - 96.9	42.6 - 492	14.2 - 70.3	21.0 - 59.4	54.9 - 121	52.9 - 123
converted mean E	COMBINED		COMBINED				COMBINED	
	0.017		0.025				0.031	
error range (1σ)	0.004 - 0.063		0.006 - 0.100				0.021 - 0.046	

3.2 Comparing E in the glaciated and unglaciated NEUS

Statistical comparisons of the regions over which E is measured, by measurement type, give a sense of the impact of glaciation on the measurement types and whether glaciated E is lower than unglaciated E , as hypothesized.

3.2.1 Stream gauging and reservoir sedimentation (last century E)

One hundred sixty-five stream gauging erosion rates were compiled: 56 glaciated; 109 unglaciated (Figure 3.2). The mean E for glaciated watersheds is 0.014 mm/yr, and unglaciated is 0.019 mm/yr, a difference of about 36% (Table 3.1). Average T of measurement for glaciated rates are 6.0 years, and 9.3 years for unglaciated. Glaciated E spans four orders of magnitude, and unglaciated rates span five (Figure 3.3).

Sixty E values were compiled from studies of reservoir sedimentation: 31 glaciated, 29 unglaciated. E means are 0.012 mm/yr for glaciated; 0.055 mm/yr for unglaciated (Table 3.1). Unglaciated mean E is over 300% greater than glaciated mean E . Measurement timescales (time since dam construction) average 48.8 years in the unglaciated region, and 23.9 years in the glaciated. Glaciated reservoir sedimentation rates span three orders of magnitude, with unglaciated spanning four (Figure 3.4).

Plotted on logarithmic-scale histograms and analyzed for statistical similarity, stream gauging E does not vary considerably between regions (Figure 3.3). Two-tailed z-tests yield one significant (≤ 0.05) and one insignificant p-value (Table 3.2). The null hypothesis ($h = 0$) posits that the data in the first category can be hypothesized to be described by the mean and 1σ error of the second. In this case, the values of h_1 and p_1 (the glaciated population compared with the unglaciated) indicate that the null hypothesis is supported, although the p-value is only slightly above 0.05 (Table 3.2). Values of h_2 (1) and p_2 (0.012) indicate that the null hypothesis can be

rejected, and that the unglaciated population is significantly different from the glaciated based on its distribution.

Reservoir sedimentation rates are more disparate by region (Figure 3.4). Z-tests return significant results for both glaciated and unglaciated populations, with p-values less than 0.05 (Table 3.2). The null hypothesis can be rejected, with unglaciated E significantly higher than glaciated. When stream gauging and reservoir sedimentation E samples are combined (hereafter referred to as last century E) to represent all data that span last century timescales, the unglaciated mean is significantly higher than glaciated (Figure 3.5; Table 3.2). The highest E appears to be in areas close to Chesapeake Bay and the Atlantic coast in Maryland and southern New Jersey (Figure 3.2).

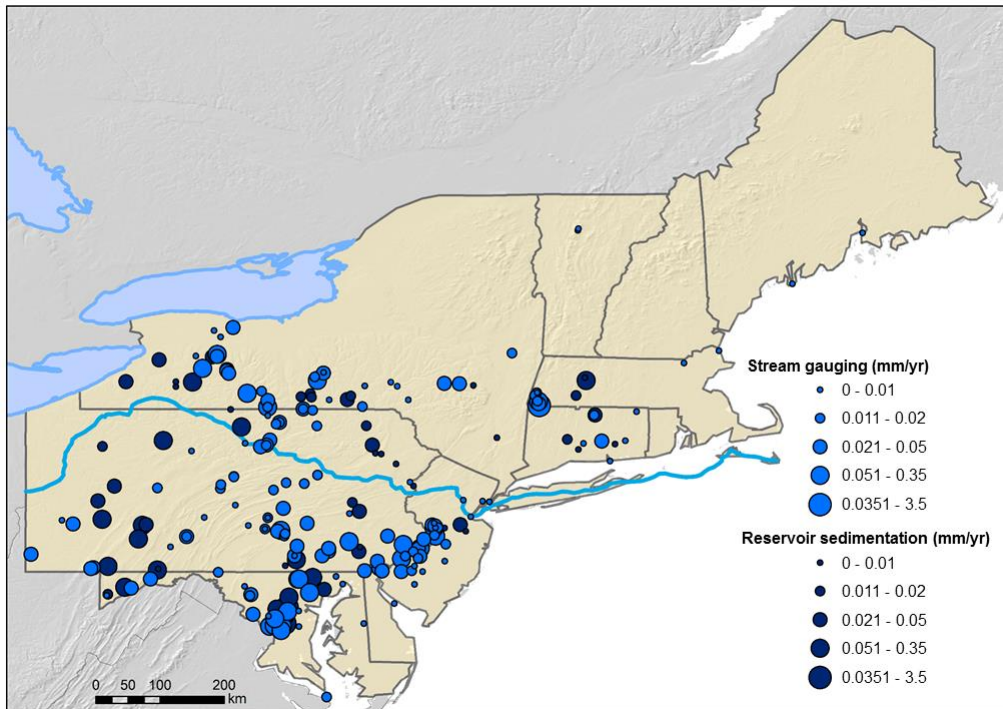


Figure 3.2 Spatial distribution of last century E .

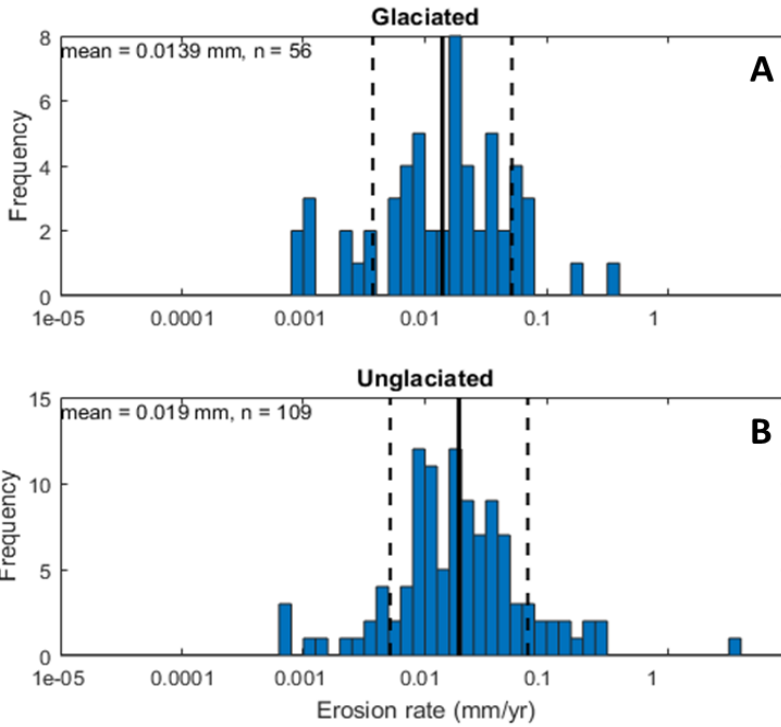


Figure 3.3 Log-scale histograms of stream gauging E by region. Z-test results: $h_1 = 0$; $h_2 = 1$.

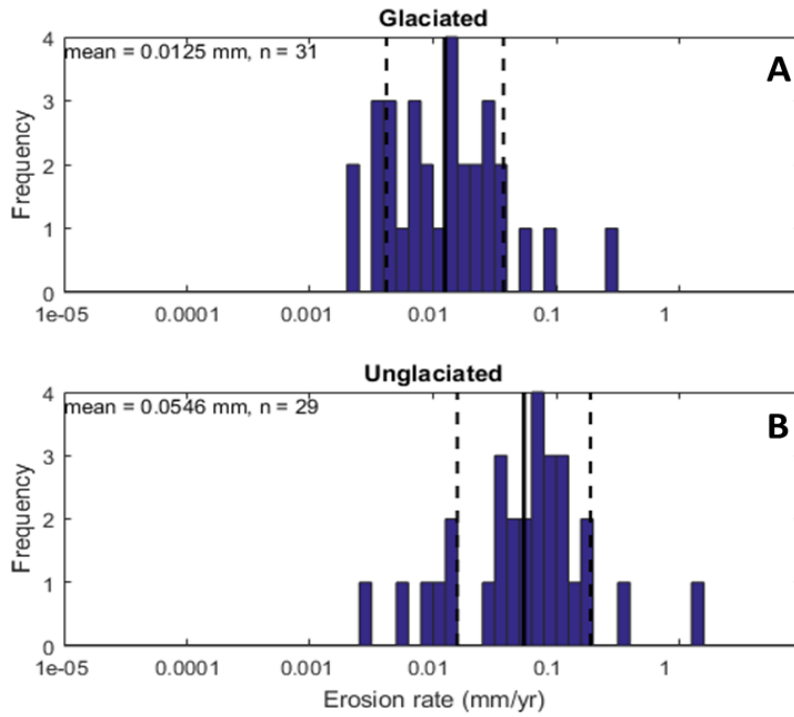


Figure 3.4 Log-scale histograms of reservoir sedimentation E by region. Z-test results: $h_1 = 1$; $h_2 = 1$.

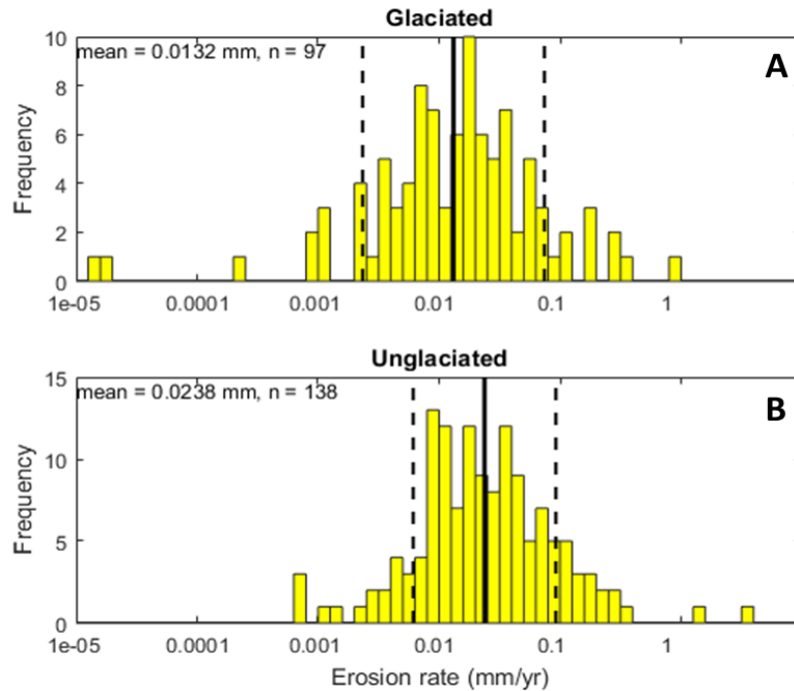


Figure 3.5 Log-scale histograms of last century E (stream gauging and reservoir sedimentation combined) by region. Z-test results: $h1 = 1$; $h2 = 1$.

Table 3.2 H and p-values for z-tests between spatially compared record types ($h1$ and $p1$ indicate the likelihood that the glaciated population can be described by the mean of the unglaciated population; $h2$ and $p2$ indicate the opposite). H values of 1 indicate that the null hypothesis – that the mean of one population can describe the other – is not supported, with $p \leq 0.05$, and the populations can be considered statistically different.

	h1	h2	p1	p2
Stream gauging	0	1	0.070	0.012
Reservoir sedimentation	1	1	4.11×10^{-11}	3.47×10^{-13}
Last century	1	1	1.79×10^{-5}	5.99×10^{-5}
Late Quaternary	0	0	0.23	0.16
Geologic	0	0	0.83	0.91

3.2.2 Lake sedimentation and cosmogenic nuclides (late Quaternary E)

Twenty-four erosion rates were compiled from lakes in glaciated New York and New England (Figure 3.6), with a mean E of 0.012 mm/yr and an average deposition timescale of 8,170 years, given by pollen, ^{14}C , ^{210}Pb , and/or ^{137}Cs dating (Table 3.1). Seventy-nine erosion rates were compiled from concentrations of ^{10}Be in stream sediments from drainage basins across Pennsylvania. The mean E for these cosmogenic nuclide-derived rates is 0.013 mm/yr, with an average timescale of 1.37×10^5 years, given by dividing the erosion rate by the attenuation depth of cosmogenic ^{10}Be .

Both distributions are relatively constrained, spanning only three orders of magnitude (Figure 3.7). Although they are not directly comparable, given the different methods used to acquire E between the two regions, their distributions are remarkably similar, with a percent difference of their means at just 8%. Z-tests return values that do not allow the null hypothesis to be rejected, with p-values of 0.23 (lake sedimentation) and 0.16 (cosmogenic nuclides) (Table 3.2).

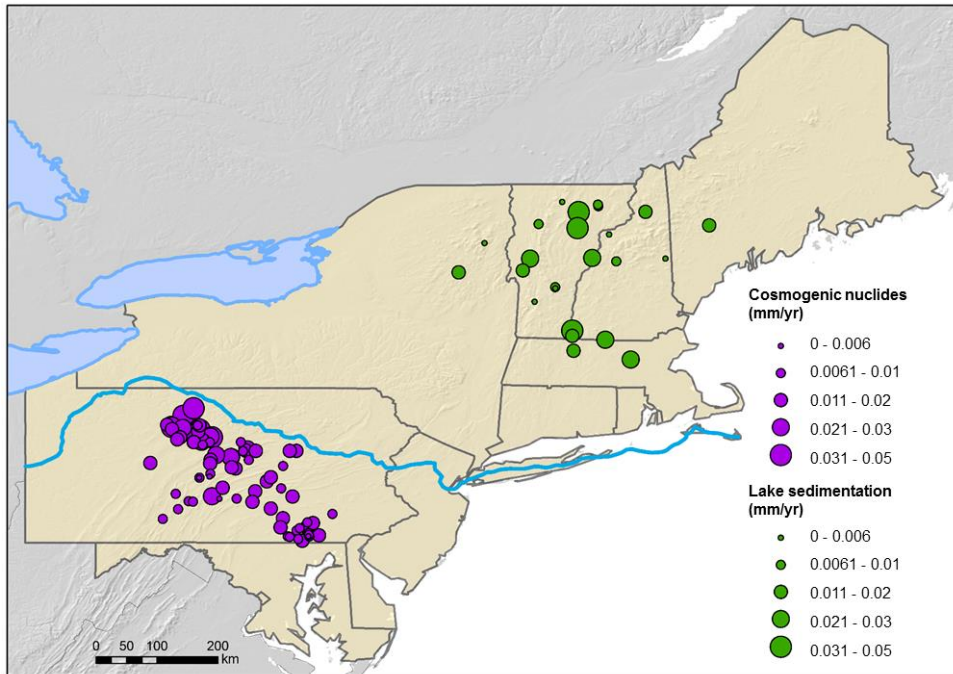


Figure 3.6 Spatial distribution of late Quaternary *E* (lake sedimentation and cosmogenic nuclides).

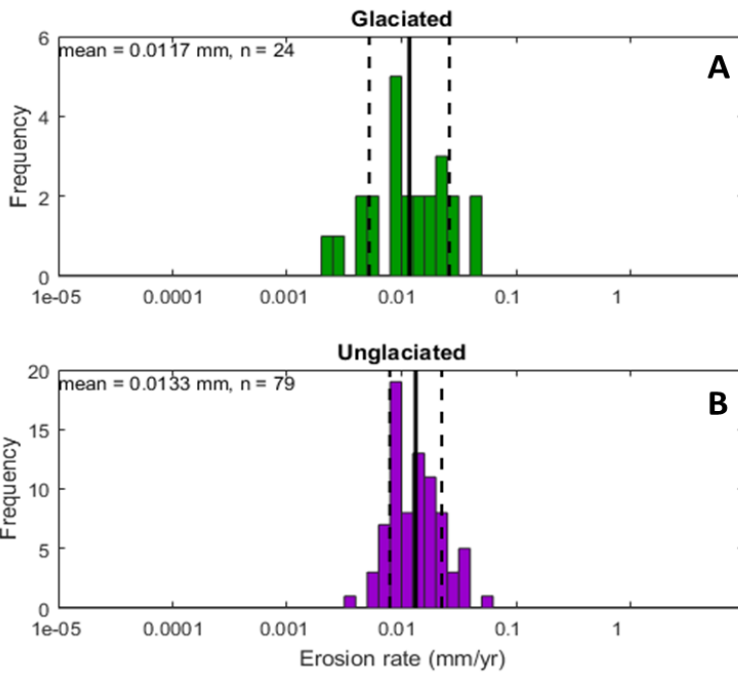


Figure 3.7 Log-scale histograms of *E* for lake sedimentation (A) and cosmogenic nuclides (B). Z-test results: $h_1 = 0$; $h_2 = 0$.

3.2.3 Thermochronology (geologic E)

Thermochronology E comprises the largest dataset, with 222 glaciated and 50 unglaciated observations (Figure 3.8). Glaciated mean E is 0.031 mm/yr, and unglaciated is 0.030 mm/yr (Table 3.2), a difference of only 3%. The average timescale is longer in the unglaciated region, with 2.24×10^8 years compared with 1.28×10^8 years. Timescales are given by radiometric dating of the minerals (usually apatite or zircon) used in thermochronologic analysis.

Distributions of E in both regions span only two orders of magnitude, the most constrained of any record type (Figure 3.9). Z-tests return values indicating that any difference between the populations can be considered insignificant, with p-values of 0.83 for glaciated and 0.91 for unglaciated (Table 3.2).

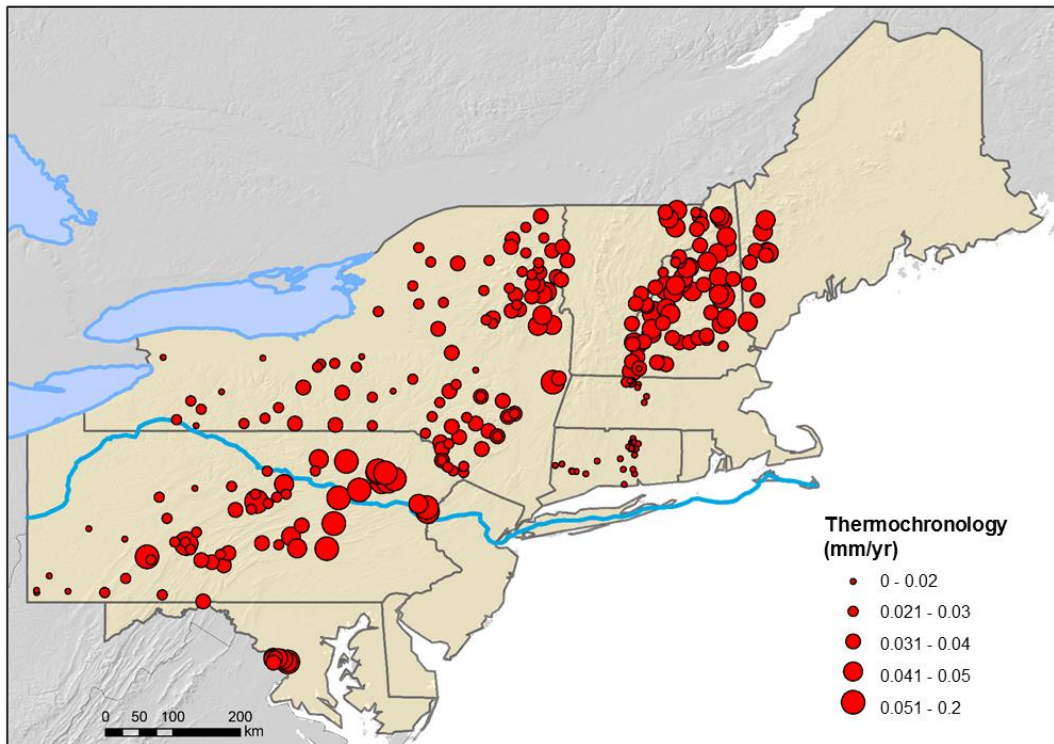


Figure 3.8 Spatial distribution of geologic E (thermochronology).

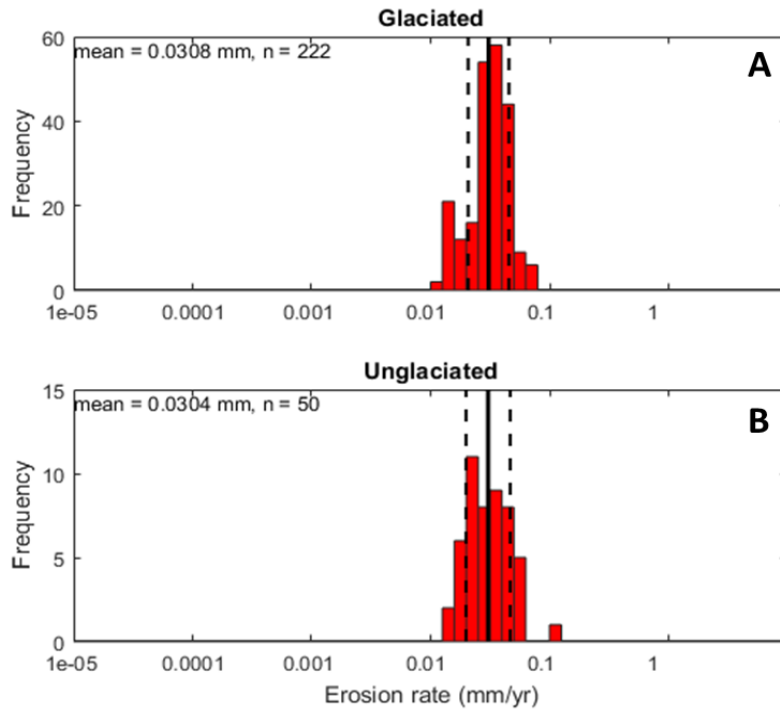


Figure 3.9 Log-scale histograms of geologic E (thermochronology) by region. Z-test results: $h_1 = 0$; $h_2 = 0$.

3.3 Comparing E across erosional timescales

Statistical comparisons of the timescales over which E is measured (as given by stream gauging and reservoir sedimentation, or last century E ; lake sedimentation or cosmogenic nuclides, or late Quaternary E ; and thermochronology, or geologic E) give a sense of temporal impact on the measurements, and whether last century E is significantly higher than longer-timescale E in the formerly glaciated and unglaciated regions of the NEUS, as hypothesized.

3.3.1 *Glaciated region*

Three populations were compared from the glaciated region: last century, lake sedimentation, and thermochronology E . The distributions and means of last century versus late Quaternary E (here, lake sedimentation) in the glaciated region are remarkably similar, with late Quaternary only slightly lower (Figure 3.10; Table 3.1). Z-tests show no significant difference between the two datasets, with p-values of 0.16 and 0.74 for last century E and lake sedimentation E , respectively (Table 3.3), indicating that the null hypothesis (that the data in the first population can be described by the distribution and mean of the second) is upheld. Thermochronology mean E , however, is significantly higher than either of the populations of shorter timescale E (Table 3.1; Table 3.3), and the null hypothesis fails. It is important to note that the distributions of both lake sedimentation and thermochronology fall within the range of last century E (Figure 3.10).

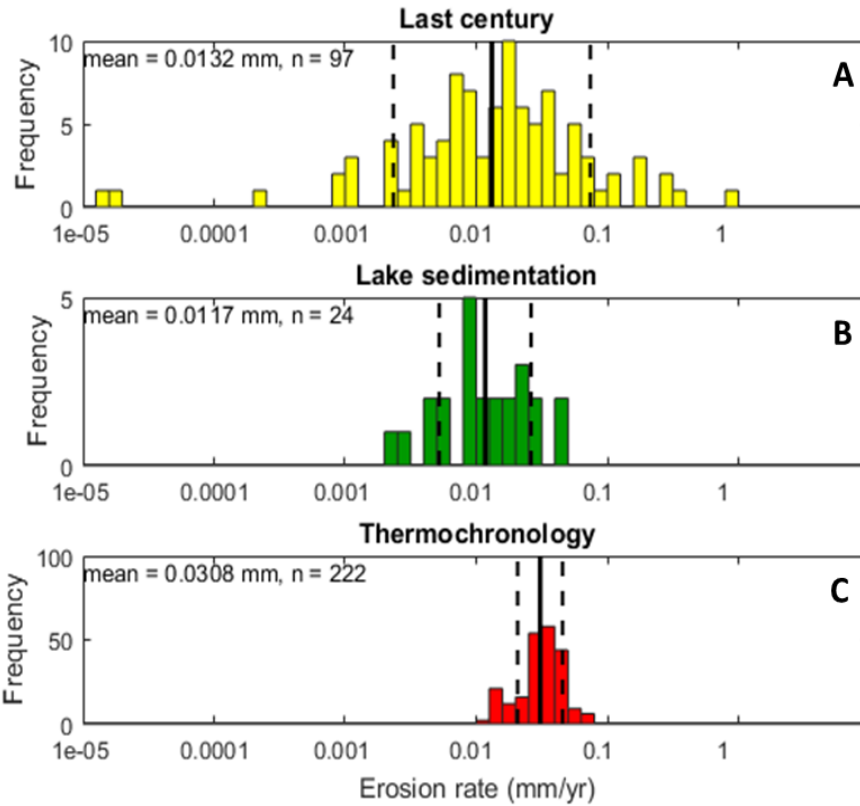


Figure 3.10 Log-scale histograms of E by record type (shortest timescale to longest) for the glaciated region.

Table 3.3 H and p-values for z-tests between record types in the glaciated region (h1 and p1 indicate the likelihood that the first listed population can be described by the mean of the second population; h2 and p2 indicate the opposite). H values of 1 indicate that the null hypothesis – that the mean of one population can describe the other – is not supported, with $p \leq 0.05$.

	h1	h2	p1	p2
Last century E vs. lake sedimentation E	0	0	0.16	0.74
Lake sedimentation E vs. thermochronology E	1	1	1.83×10^{-32}	3.96×10^{-73}
Thermochronology E vs. last century E	1	1	1.74×10^{-13}	9.36×10^{-97}

3.3.2 Unglaciaded region

Populations of last century, cosmogenic nuclide, and thermochronology E were compared in the unglaciaded region. Of the three populations, cosmogenic nuclides show the lowest mean E , with last century mean E only slightly lower than that of thermochronology (Figure 3.11). Z-tests suggest cosmogenic nuclide E is significantly lower than both other record types (Table 3.4). Thermochronology and last century E yield two different z-test results, which indicates that the thermochronology distribution may be described by the mean and standard deviation of last century E , although the opposite is not true (when comparing last century E with thermochronology, the null hypothesis is supported) (Table 3.4). Again, the distributions of both thermochronology and cosmogenic nuclide E fall within the range of last century E (Figure 3.11).

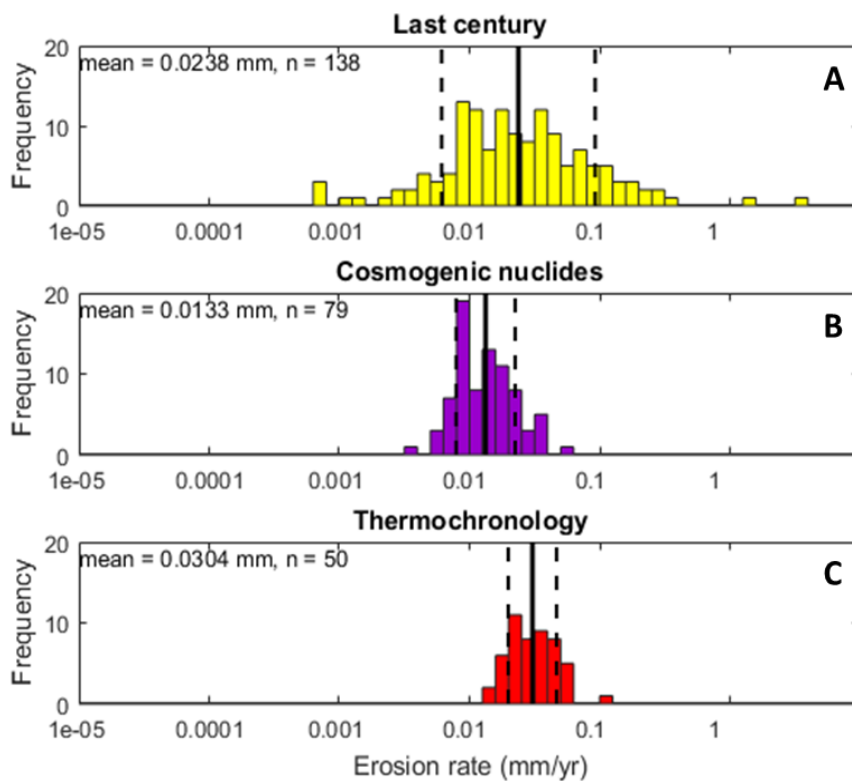


Figure 3.11 Log-scale histograms of E by record type (shortest timescale to longest) for the unglaciaded region.

Table 3.4 H and p-values for z-tests between record types in the unglaciated region. H1 and p1 indicate the likelihood that the first listed population can be described by the mean of the second population; h2 and p2 indicate the opposite. H values of 1 indicate that the null hypothesis – that the mean of one population can describe the other – is not supported, with $p \leq 0.05$.

	h1	h2	p1	p2
Last century <i>E</i> vs. cosmogenic nuclide <i>E</i>	1	1	1.27×10^{-38}	1.48×10^{-4}
Cosmogenic nuclide <i>E</i> vs. thermochronology <i>E</i>	1	1	1.77×10^{-66}	6.10×10^{-29}
Thermochronology <i>E</i> vs. last century <i>E</i>	0	1	0.20	9.61×10^{-12}

3.3.3 Combined

Here, all data are considered in order to determine whether *E* is timescale-dependent, regardless of glacial history. Comparing the glaciated and unglaciated results above, the late Quaternary timescales consistently yield the lowest mean *E*, with geologic *E* (thermochronology) highest and last century *E* intermediate, although they vary regionally by differing degrees. With glaciated and unglaciated data combined, erosional differences between timescales appear negligible in the NEUS (Figure 3.12; Table 3.1). This suggests little timescale dependence on *E*, which does not support the hypothesis that more recent records measured over shorter timescales will yield higher *E*. Reservoir sedimentation yields the largest range in *E*, followed by stream gauging, lake sedimentation, cosmogenic nuclides, and thermochronology (Figure 3.13). Thus, there appears to be a timescale dependence on the range of the distributions, with longer timescales yielding smaller ranges in *E*.

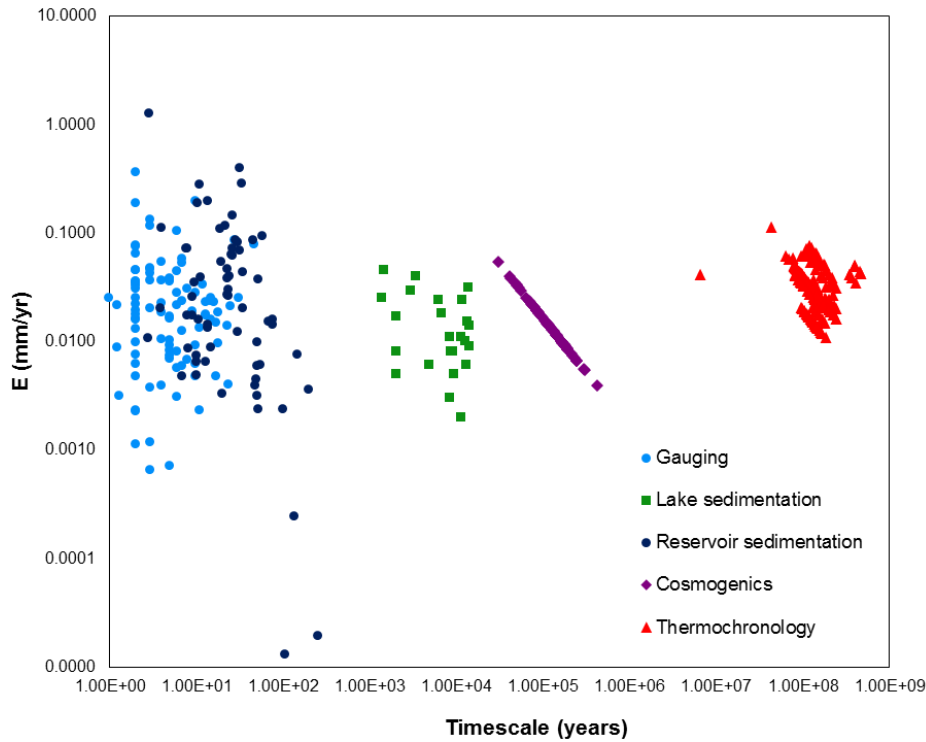


Figure 3.12 E versus T for all points, by record type. Cosmogenic nuclide data fall along a straight line because attenuation depth of ^{10}Be (165 cm below the surface; Reuter, 2005) was divided by erosion rate in order to obtain the timescale over which erosion occurred.

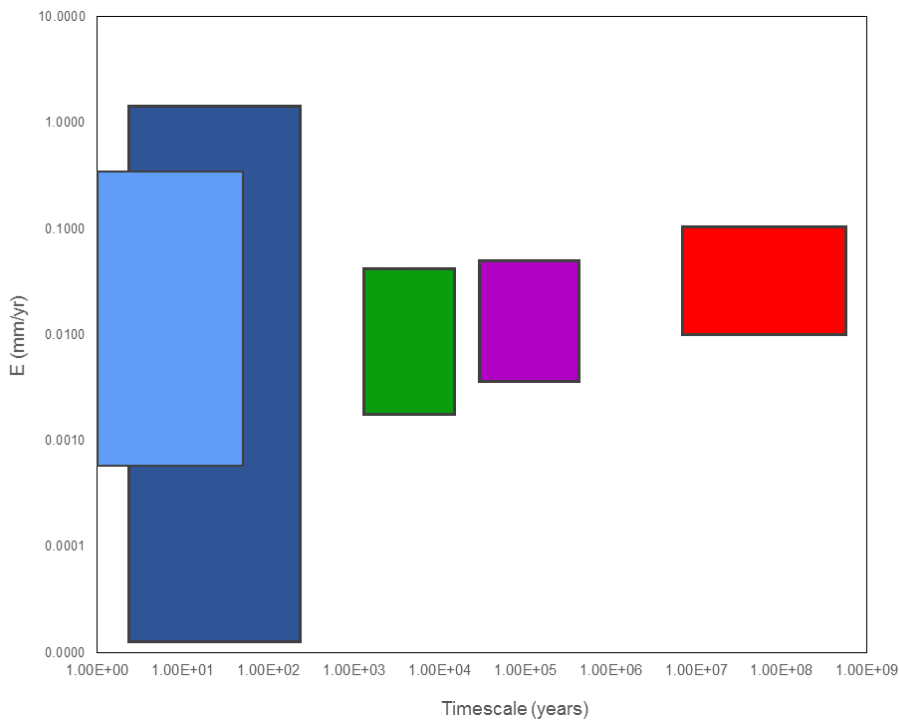


Figure 3.13 Comparison of E by record type. Boxes represent the ranges of erosion rates and timescales, with timescale of measurement represented by their width.

3.4 Drainage basin area (A_B) as a control on E

Erosion rate was hypothesized to have a negative relationship with A_B , as larger basins tend to have more places to store sediment – on terraces and floodplains and behind dams, for example – and will therefore reflect a lower sediment delivery ratio. A total of 306 points had available A_B from stream gauging, reservoir sedimentation, lake sedimentation, and cosmogenic nuclide studies. Stream gauging studies provided about half of the total available points. Thermochronology erosion rates represent points, not basin-wide averages, and were therefore excluded from the dataset.

All E points were plotted against drainage area with a least-squares power-law regression. Only stream gauging exhibits a significant, albeit weak, correlation, with $R^2 = 0.11$ (Figure 3.14a). Reservoir sedimentation displays an insignificant relationship, with R^2 of 0.012 and a p-value of 0.374 (Figure 3.14b), contrary to Ahamed's (2014) results for reservoir sedimentation Y_s in the entire eastern United States, which exhibit a weak negative correlation between Y_s and drainage area ($R^2 = 0.09$, $p < 0.001$). Lake sedimentation and cosmogenic nuclide E both display insignificant relationships with drainage area (Figure 3.14c; 3.14d). When points from all record types are plotted together, a significant, but weak negative relationship appears between E and drainage area, with $R^2 = 0.013$ and $p = 0.043$ (Figure 3.14e).

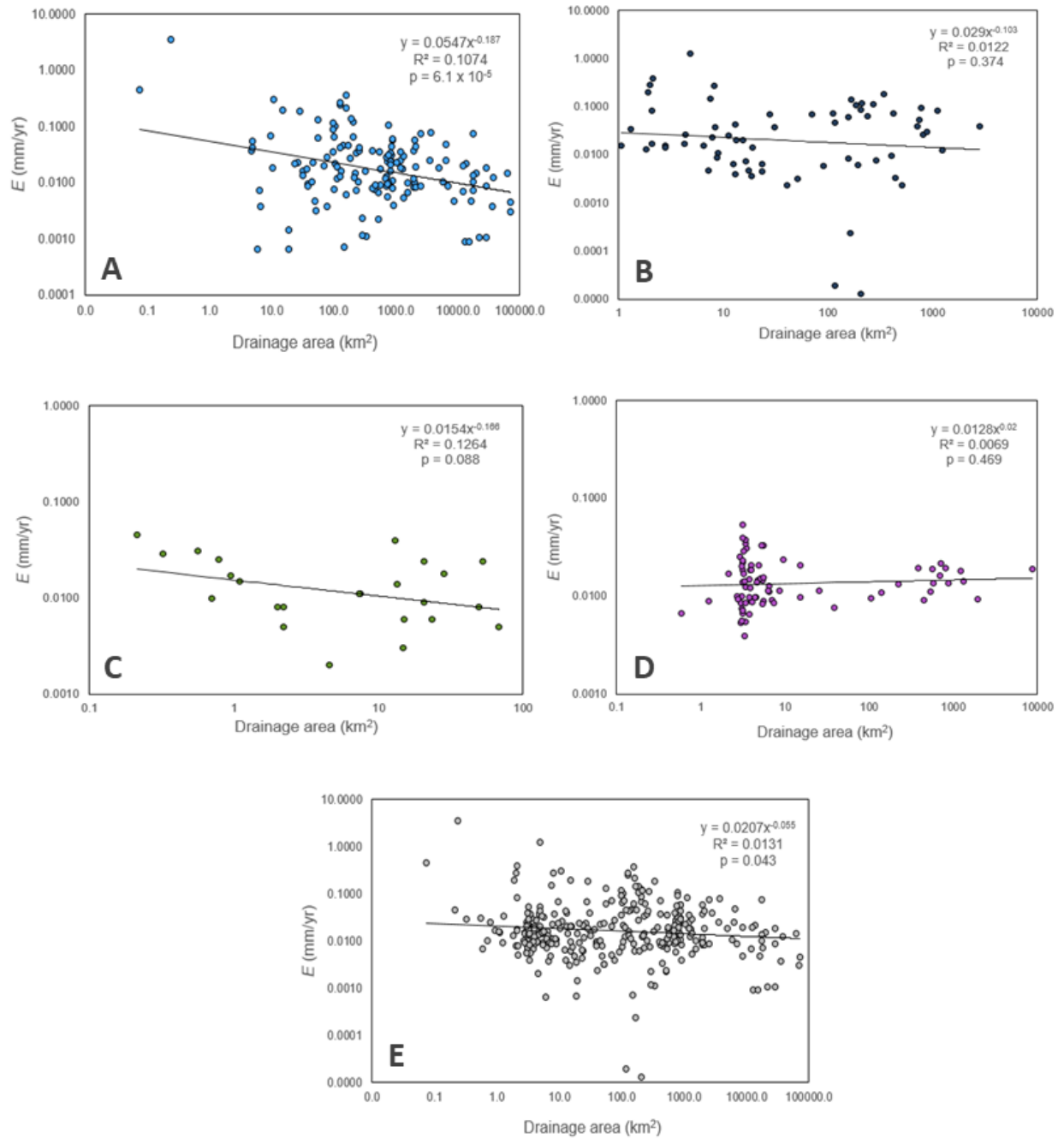


Figure 3.14 Logarithmic plots of E versus drainage basin area for all points with available area data (excluding thermochronology). A: Stream gauging; B: Reservoir sedimentation; C: Lake sedimentation; D: Cosmogenic nuclides; E: Combined points.

4. DISCUSSION

4.1 Comparing NEUS E with global E

Last century timescales in the NEUS yield a similar order of erosion rate (E) estimates to those derived from global compilations of fluvial sediment fluxes (Table 1.1; Table 3.1). An average of 0.017 mm/yr from stream gauging and 0.025 mm/yr from NEUS reservoir sedimentation are lower than global E of 0.069 mm/yr (Summerfield and Hulton, 1994) and 0.110 mm/yr (Milliman and Farnsworth, 2011), but within range when 1σ error is taken into account (Table 3.1).

There is a wider range of previously published global erosion estimates for geologic timescales compared with those compiled from the NEUS (Table 1.1). Sources use a wide variety of methods in their measurements, from estimating volumes of Phanerozoic sedimentary rocks (0.016 mm/yr; Wilkinson and McElroy, 2007) to combined thermochronologic and cosmogenic nuclide data (0.036 mm/yr; Montgomery, 2007) to basin-wide E derived from concentrations of ^{10}Be (0.218 mm/yr; Portenga and Bierman, 2011). Erosion rates in the NEUS derived from ^{10}Be are the lowest of all the record types (0.013 mm/yr), second only to lake sedimentation (0.012 mm/yr), with average ^{10}Be E one order of magnitude lower than the global average given by Portenga and Bierman (2011) (Table 1.1; Table 3.1). This suggests relative stability of sediment movement over late Quaternary timescales in the NEUS.

Erosion rate averages in the NEUS given by thermochronology are an order of magnitude lower than global averages given by Portenga and Bierman (2011) and Montgomery (2007), which include data from tectonically active regions. Thus, while thermochronology yields the highest overall E in the NEUS, geologic erosion rates from the NEUS are low relative to global averages.

4.2 Comparing E in the glaciated and unglaciated NEUS

4.2.1 Last century E : Stream gauging and reservoir sedimentation

Hypothesis 1, that E would be lower in the glaciated NEUS than the unglaciated NEUS over last century timescales due to a more limited mobile sediment supply, is supported, with unglaciated mean E nearly twice that of glaciated mean E and both z-tests returning a significant result (Figure 3.5; Table 3.2). Additionally, both record types exhibit higher E in the unglaciated region. Reservoir sedimentation E in particular exhibits a noteworthy disparity between regions, which may tip the overall result towards significantly higher E in the unglaciated region.

When last century E is split into its respective record types, the spatial hypothesis is not supported by stream gauging records. Although average E is higher in the unglaciated region than glaciated (0.019 mm/yr vs. 0.014 mm/yr, respectively; Table 3.1), results of the z-tests return only one rejection of the null hypothesis; the unglaciated population cannot be described by the mean and standard deviation of the glaciated population, but the opposite is not true (Table 3.2). This suggests that short-term erosion is relatively comparable between the two regions, perhaps indicating that similar modern climate and post-settlement land use histories are more influential than the regions' respective glacial histories.

Spatially, it appears as though the highest stream gauging E occurs along the Appalachian Fall Line, where river slopes decrease as they flow into the Atlantic coastal plain (Figure 3.2). However, there are also more measurements clustered tightly in this area, so the appearance of high E may instead be indicative of a larger sampling effort. The lack of stream gauging E in northern New England (Vermont, New Hampshire and Maine) is also noteworthy, as measurements tend to occur where there is a need for management or mitigation; an increased

sampling effort in these states might lower glaciated stream gauging E , possibly strengthening the probability of rejection of the null hypothesis.

The difference in mean reservoir sedimentation E between regions is more evident, with a glaciated mean E of 0.012 mm/yr and an unglaciated mean of 0.055 mm/yr and both z-tests yielding a significant result (Table 3.1; Table 3.2). The greater disparity in regional reservoir sedimentation than stream gauging E warrants discussion, as one might expect both last century methods of measurement to exhibit a similar difference.

Average timescales over which stream gauging Y_s is measured are higher in the unglaciated region than glaciated, and approximately twice as many unglaciated stream gauging erosion rates are available (Table 3.1), likely a result of extensive research and funding related to issues with sedimentation in the Chesapeake Bay. Reservoir sedimentation E is measured over considerably longer timescales than stream gauging, with glaciated and unglaciated regions incorporating sedimentation over averages of 48.8 and 23.9 years, respectively (Table 3.1). Contrastingly, stream gauging E is measured over an average of 6.0 and 9.3 years in the glaciated and unglaciated regions. Although still compiled over the last century, decades-long records will be more effective at incorporating large magnitude flood sedimentation than those measured over several years, therefore potentially more representative of long-term erosion. The longer the averaging timescale, however, the more likelihood of lower E , as sediment may be subject to resuspension and/or compaction; over long timescales, the sediment record will also incorporate more hiatuses in sedimentation (Sadler, 1981).

There are a number of problems with treating stream gauging and reservoir sedimentation E estimates as long-term rates, the most important of which is the difficulty of integrating events of all magnitudes into a short record. Fluvial sediment deposition tends to happen in short pulses,

with long periods of inactivity between (Sadler and Jerolmack, 2014). Thus, records shorter than about five years, of which there are many in this dataset (particularly in the glaciated region), may not represent longer-term averages (Summerfield and Hulton, 1994). Milliman and Farnsworth (2011) cite a 50% error in measuring suspended sediment loads at gauging stations; Walling (1977) assigns annual stream gauging rating curves up to 280% error. The error inherent in the measuring and rating process may affect average E , as the difference between regional stream gauging E is only 36%. Additionally, reservoir sedimentation rates have been corrected for the trapping effect of upstream dams by subtracting out drainage area contributing to upstream reservoirs (Ahamed, 2014). A similar correction has not been made for stream gauging data. The wide variance in stream gauging and reservoir sedimentation distributions, especially when compared with those from longer averaging timescales (Figure 3.10, Figure 3.11), may be partially explained by the above factors. Differences in measurement technique and length of record, when combined with stochastic flood events, lead to greater ranges in E ; longer records and standardized methods would go a long way in reducing error.

The influence of drainage area on E is most pronounced with stream gauging data, with a significant inverse relationship (Figure 3.14a), establishing the importance of sediment sinks in large watersheds while also calling into question whether gauging stations in those watersheds are capturing representative E . Reservoir sedimentation, however, does not exhibit a statistically significant relationship with drainage area (Figure 3.14b), in contrast with the results of Ahamed's (2014) analysis. Estimates of E from reservoirs in the ResSed database are taken largely from upland dams with an average drainage area of 220 km², and very few from main stem rivers. The buffering capacity of floodplains in large drainage basins may have important effects on the magnitude of E measured from stream gauging, as rates come from basin sizes

ranging from 0.1 to 71,000 km², with an average basin area of 4600 km² (Appendix 1). This may decrease apparent E with respect to stream gauging measurements, and therefore introduce more uncertainty into this dataset.

4.2.2 Late Quaternary E: Lake sedimentation and cosmogenic nuclides

To the extent that it can be applied, the spatial hypothesis is not supported when comparing lake sedimentation (glaciated) and cosmogenic nuclide (unglaciated) E . Their distributions are remarkably similar, despite their disparate glacial histories and averaging timescales (Figure 3.7; Table 3.1). Z-tests return no significant difference in their populations, even though lake sedimentation occurred post-glaciation (as New England lakes were created after deglaciation) and erosion measured by cosmogenic nuclides occurred over late Pleistocene timescales, during which E would have been influenced by periglacial processes and subsequent post-glacial warming. Both exhibit ranges over three orders of magnitude, more constrained than the stream gauging and reservoir sedimentation distributions. Whether the similarity between the methods is a reflection of the comparability of late Quaternary timescale processes is a question that may not be resolved, given the methods intrinsic to the ways they are measured. Still, their resemblance points to their relatively low levels of erosion spanning timescales of 10^3 to 10^5 years.

4.2.3 Geologic E: Thermochronology

A large proportion of the thermochronologic work completed in the NEUS in the last 30 years has been done by Mary Roden-Tice, thus the collected erosion estimates are dominated by her and her collaborators (Appendix 1). Rates are relatively evenly spread across the NEUS, although there is a clear preference for work in New Hampshire's White Mountains, and a lack

of data in Rhode Island, New Jersey, and Maryland (Figure 3.8). The number of points in the glaciated region exceeds those in the unglaciated region by about five to one. Despite this imbalance, the two distributions are remarkably similar, with virtually the same average E , a difference of only 0.001 mm/yr (Figure 3.9; Table 3.1). Z-tests return no significant difference between the populations.

Although the regions have differing glacial histories, the timescale over which glaciation would have an effect on E is relatively short compared to their averaging timescales, and their geologic histories would be more influential on their respective rates of erosion. The central Appalachians were primarily formed by the Alleghenian orogeny during the Mesozoic era. The White Mountains were formed by the passage of the North American Plate over the New England hotspot in the early Cretaceous period (McKeon et al., 2014), with the Paleozoic Acadian orogeny doing the majority of the mountain-building over most of New England. The timescales over which E is measured may reflect the relative youth of the White Mountains; on average, samples from the unglaciated region exceed the age of the glaciated samples by about 100 million years (Table 3.1).

Relatively high E over tectonic timescales may reflect the importance of the period during which mountain building was taking place: rapid uplift would have resulted in equally rapid erosion as basins attempted to reach steady-state conditions. In high-gradient landscapes, landsliding becomes more frequent as tectonic uplift occurs, linking E and slope (Montgomery and Brandon, 2002). Given that the Appalachian landscape likely experienced millions of years of active uplift, this may have affected the resulting exhumation rates recorded by thermochronology in the NEUS.

4.3 Comparing E across erosional timescales

The temporal hypothesis tests whether there is a timescale dependence on erosion in the NEUS; namely, whether there is an increase in E from geologic and late Quaternary rates to last century rates. Overall, there is a striking similarity between all reported mean E , even those considered statistically disparate. In the glaciated region, there is statistical similarity between lake sedimentation and last century E (Figure 3.10; Table 3.3), suggesting that the magnitude of modern erosion in the glaciated NEUS has not changed appreciably since ca. 10,000 years ago. In the unglaciated region, last century E is statistically greater than cosmogenic nuclide E (Figure 3.11; Table 3.4), but only when including reservoir sedimentation E ; stream gauging E is considerably lower, and ultimately more comparable to cosmogenic nuclide E , with 0.019 and 0.013 mm/yr, respectively (Table 3.1).

Geologic E from thermochronologic denudation estimates is consistently higher than all other timescales in the NEUS. A possible explanation is the relative importance of orogenic activity in the region, as mountain building necessitates subsequent unroofing. Thermochronologic samples incorporate E from as far back as the Ordovician period, with mean T of unglaciated thermochronologic samples at 224 m.y., and 128 m.y. for glaciated (Table 3.1). These E estimates likely encompass the time in which the Alleghenian and Acadian orogenies were occurring in the NEUS. The exception to the dominance of thermochronologic E is in the unglaciated region, where it is similar to last century E ; z-tests returned one significant and one insignificant result (Table 3.4). Again, the magnitude of reservoir sedimentation E in the unglaciated region is likely responsible for their being roughly equal: thermochronology mean E is nearly twice that of stream gauging, but reservoir sedimentation is nearly twice that of thermochronology (Table 3.1).

Timescale dependence on E does not appear to exist in the NEUS, with all mean E well within one order of magnitude (Table 3.1). This is a contrasting result from those of Reuter (2005) and Montgomery (2007), who found order-of-magnitude increases from background to modern E , and Kirchner et al. (2001) and Covault et al. (2013), who found significant decreases in modern compared to cosmogenic E . There does appear to be timescale dependence regarding the distributions of the methods, however; in all cases, thermochronologic E spans the smallest range, followed by late Quaternary E ; last century E spans five and six orders of magnitude in the unglaciated and glaciated regions, respectively (Figures 3.10 and 3.11).

A noteworthy absence in this study is the assessment of E immediately post-European settlement in the NEUS, when forest clearing was at its peak. The most recent calculation of post-settlement erosion comes from Johnson (2017), who estimates a basin-wide E of 12-37 mm in the South River watershed, Massachusetts, and E of 2-7 mm in the Sheepscot watershed in Maine. With a settlement estimate of ca. 1750 in the South River and the late 1600s in the Sheepscot, and approximately 100 years of active erosion, post-settlement E of 0.02 to 0.37 mm/yr can be calculated for the formerly glaciated NEUS. Although slightly higher, this estimate of post-settlement E is still within range of last century E in the glaciated NEUS (Figure 3.5a). Workers from Franklin and Marshall College in PA have recently estimated similar post-settlement E , with 0.7 to 2.3 cm (0.07-0.23 mm/yr) of soil erosion from the Indian Run, Chiques Creek, and Big Beaver Creek watersheds in unglaciated PA (Snyder et al., 2017). Previous estimates of post-settlement E in the unglaciated NEUS are higher: they range from 7.6 to 30.5 cm over roughly the same period (Bennett and Chapline, 1928; Hartman and Wooten, 1935; Happ, 1945; Overstreet et al., 1968; Costa, 1975). These estimates are an order of magnitude

higher than any E estimates in this study, and indicate the potential importance of human activity over relatively short timescales, even if their effects do not necessarily continue into the present.

5. SUMMARY AND CONCLUSIONS

This study compares published records of erosion rates obtained from stream gauging, reservoir sedimentation, lake sedimentation, cosmogenic nuclides, and thermochronology in the NEUS in order to determine whether there is a measurable effect of glacial history (spatial hypothesis) and timescale (temporal hypothesis) on the movement of sediment in the NEUS. All measurements were converted to erosion rate (E ; mm/yr) and sediment yield (Y_s ; t km⁻² yr⁻¹) and subjected to statistical z-tests in order to determine whether their distributions were similar. E was compiled for 499 study sites for all five record types in their respective regions, the means of which were well within one order of magnitude (range of 0.012 to 0.055 mm/yr).

The spatial hypothesis, that E and Y_s are lower in the glaciated region than the unglaciated region over last century (stream gauging; reservoir sedimentation) timescales, was supported by reservoir sedimentation E , which exhibits a significantly higher mean in the unglaciated region (0.055 mm/yr) over the glaciated (0.012), but was not supported by stream gauging E . The large size of the stream gauging basins, the relatively short timescales of measurement, and the spatial disproportion of the measurements may confound the results; an ideal dataset would include estimates from smaller basins, longer records, and a more even spatial distribution to more accurately represent E in this region.

Contrary to the conclusions of other researchers, there appears to be neither an increase or a decrease in E when comparing temporal records. Thermochronology E is highest in both regions, averaging 0.031 mm/yr, with reservoir sedimentation closest at an average of 0.025 mm/yr, and the rest of the rates between 0.01 and 0.02 mm/yr. This may suggest that, although land use change can affect E over short timescales in the NEUS, it is not yet a match for the tectonic processes that average over tens of millions of years. In general, however, the

similarities in mean E between timescales, as well as the range of their distributions, point to the relative stability of E in the NEUS over the timescales examined.

REFERENCES

- Ahamed, A., 2014, Geomorphic and Land Use Controls on Sediment Yield in Eastern USA: M.S. thesis, Boston College, Chestnut Hill, MA.
- Ahnert, F., 1970, Functional relationships between denudation, relief, and uplift in large mid-latitude drainage basins: *American Journal of Science*, v. 268, p. 243-163.
- Allmendinger, N. E., Pizzuto, J. E., Moglen, G. E., and Lewicki, M., 2007, A sediment budget for an urbanizing watershed, 1951-1996, Montgomery County, Maryland, U.S.A.: *Journal of the American Water Resources Association*, v. 43, no. 6, p. 1483-1498.
- Anderson, P. W., and George, J. R., 1966, Water-Quality Characteristics of New Jersey Streams: Geological Survey Water-Supply Paper 1819-G, 48 p.
- Bell, M., and Laine, E. P., 1985, Erosion of the Laurentide Region of North America by Glacial and Glaciofluvial Processes: *Quaternary Research*, v. 23, no. 2, p. 154-174.
- Bennett, H. H., and Chapline, W. R., 1928, Soil erosion: A national menace: U.S. Department of Agriculture Circular #33, 36 p.
- Bierman, P. R., and Montgomery, D. R., 2014, *Key Concepts in Geomorphology*, W. H. Freeman and Company, 500 p.
- Bierman, P. R., and Nichols, K. K., 2004, Rock to Sediment – Slope to Sea with ^{10}Be – Rates of Landscape Change: *Annual Reviews in Earth and Planetary Science*, v. 32, p. 215-255.
- Bierman, P. R., and Steig, E. J., 1996, Estimating rates of denudation using cosmogenic isotope abundances in sediment: *Earth Surface Processes and Landforms*, v. 21, p. 125-139.
- von Blanckenburg, F., 2005, The control mechanisms of erosion and weathering at basin scale from cosmogenic nuclides in river sediment: *Earth and Planetary Science Letters*, v. 237, p. 462-479.
- Bormann, F. H., Likens, G. E., Siccama, T. G., Pierce, R. S., and Eaton, J. S., 1974, The export of nutrients and recovery of stable conditions following deforestation at Hubbard Brook: *Ecological Monographs*, v. 44, no. 3, p. 255-277.
- Brush, G. S., 1984, Patterns of recent sediment accumulation in Chesapeake Bay (Virginia-Maryland, U.S.A.) tributaries: *Geochronology of Recent Deposits, Chemical Geology*, v. 44, p. 227-242.
- Burbank, D. W., and Anderson R. S., 2012, *Tectonic Geomorphology*, Wiley-Blackwell, 411 p.

- Clapp, E. M., Bierman, P. R., Schick, A. P., Lekach, J., Enzel, Y., and Caffee, M., 2000, Sediment yield exceeds sediment production in arid region drainage basins: *Geology*, v. 28, no. 11, p. 995-998.
- Conrad, C. T., 2000, Spatial and temporal patterns of fluvial suspended sediment yield from Eastern North America: Ph.D thesis, Wilfrid Laurier University, Waterloo, Ontario, Canada.
- Costa, J. E., 1975, Effects of Agriculture on Erosion and Sedimentation in the Piedmont Province, Maryland: *Geological Society of America Bulletin*, v. 86, no. 9, p. 1281-1286.
- Covault, J. A., Craddock, W. H., Romans, B. W., Fildani, A., and Gosai, M., 2013, Spatial and Temporal Variations in Landscape Evolution: Historic and Longer-Term Sediment Flux through Global Catchments: *The Journal of Geology*, v. 121, no. 1, p. 35-56.
- Davis, M. B., 1969, Climatic changes in southern Connecticut recorded by pollen deposition at Rogers Lake: *Ecology*, v. 50, no. 3, p. 409-422.
- Duxbury, J., Bierman, P. R., Portenga, E. W., Pavich, M. J., Southworth, S., and Freeman, S. P. H. T., 2015, Erosion rates in and around Shenandoah National Park, Virginia, determined using analysis of cosmogenic ^{10}Be : *American Journal of Science*, v. 315, no. 1, p. 46-76.
- Edgington, D. N., Klump, J. V., Robbins, J. A., Kusner, Y. S., Pampura, V. D., and Sandimirov, I. V., 1991, Sedimentation rates, residence times and radionuclide inventories in Lake Baikal from ^{137}Cs and ^{210}Pb in sediment cores: *Nature*, v. 350, p. 601-604.
- Evans, J. K., Gottgens, J. F., Gill, W.M., and Mackey, S. D., 2000, Sediment Yields Controlled by Intrabasinal Storage and Sediment Conveyance over the Interval 1842-1994: Chagrin River, Northeast Ohio, U.S.A.: *Journal of Soil and Water Conservation*, v. 55, no.3, p. 264-270.
- Gordon, R. B., 1979, Denudation of central New England determined from estuarine sedimentation: *American Journal of Science*, v. 279, p. 632-642.
- Granger, D. E., Kirchner, J. W., and Finkel, R., 1996, Spatially averaged long-term erosion rates measured from in situ-produced cosmogenic nuclides in alluvial sediment: *The Journal of Geology*, v. 104, no. 3, p. 249-257.
- Granger, D. E., and Schaller, M., 2014, Cosmogenic nuclides and erosion at the watershed scale: *Elements*, v. 10, p. 369-373.
- Griffiths, P. G., Hereford, R., and Webb, R. H., 2006, Sediment yield and runoff frequency of small drainage basins in the Mojave Desert, USA: *Geomorphology*, v. 74, no. 1, p. 232-244.

- Hancock, G., and Kirwan, M., 2007, Summit erosion rates deduced from ^{10}Be : Implications for relief production in the central Appalachians: *Geology*, v. 35, no. 1, p. 89-92.
- Happ, S. C., 1945, Sedimentation in South Carolina Piedmont valleys: *American Journal of Science*, v. 243, no.3, p. 113-126.
- Hartman, W. A., and Wooten, H. H., 1935, Georgia land use problems: *Georgia Agricultural Experiment Station Bulletin*, no. 191, 40 p.
- Hewawasam, T., von Blanckenburg, F., Schaller, M., and Kubik, P., 2003, Increase of human over natural erosion rates in tropical highlands constrained by cosmogenic nuclides: *Geology*, v. 31, no. 7, p. 597-600.
- Hooke, R. L., 2000, Toward a uniform theory of clastic sediment yield in fluvial systems: *Geological Society of America Bulletin*, v. 112, no. 12, p. 1778-1786.
- Hovius, N., and Leeder, M., 1998, Clastic sediment supply to basins: *Basin Research*, v. 10, p. 1-5.
- Judson, S., and Ritter, D. F., 1964, Rates of Regional Denudation in the United States: *Journal of Geophysical Research*, v. 69, no. 16, p. 3395-3401.
- Kirchner, J. W., Finkel, R. C., Riebe, C. S., Granger, D. E., Clayton, J. L., King, J. G., and Megahan, W. F., 2001, Mountain erosion over 10 yr, 10 k.y., and 10 m.y. time scales: *Geology*, v. 29, no. 7, p. 591-594.
- Koppes, M. N., and Montgomery, D. R., 2009, The relative efficacy of fluvial and glacial erosion over modern to orogenic timescales: *Nature Geoscience*, v. 2, no. 9, p. 644-647.
- Langbein, W. B., and Schumm, S. A., 1958, Yield of sediment in relation to mean annual precipitation: *American Geophysical Union Transactions*, v. 39, p. 1076-1084.
- MacDonald, G. M., Beukens, R. P., and Kieser, W. E., 1991, Radiocarbon dating of limnic sediments: A comparative analysis and discussion: *Ecology*, v. 72, no. 3, p. 1150-1155.
- Matmon, A., Bierman, P. R., Larsen, J., Southworth, S., Pavich, M., and Caffee, M., 2003, Temporally and spatially uniform rates of erosion in the southern Appalachian Great Smoky Mountains: *Geology*, v. 31, no. 2, p. 155-158.
- McKeon, R. E., Zeitler, P. K., Pazzaglia, F. J., Idleman, B. D., and Enkelmann, E., 2014, Decay of an old orogen: Inferences about Appalachian landscape evolution from low-temperature thermochronology: *GSA Bulletin*, v. 126, no. 1-2, p. 31-46.
- Meade, R. H., 1969, Errors in Using Modern Stream-Load Data to Estimate Natural Rates of Denudation: *Geological Society of America Bulletin*, v. 80, p. 1265-1274.

- Meade, R. H., 1982, Sources, sinks, and storage of river sediment in the Atlantic drainage of the United States: *The Journal of Geology*, v. 90, no. 3, p. 235-252.
- Milliman, J. D., and Farnsworth, K. L., 2011, *River discharge to the coastal ocean: a global synthesis*, Cambridge University Press, 384 p.
- Milliman, J. D., and Syvitski, J. P. M., 1992, Geomorphic/Tectonic Control of Sediment Discharge to the Ocean: The Importance of Small Mountainous Rivers: *The Journal of Geology*, v. 100, no. 5, p. 525-544.
- Montgomery, D. R., 2007, Soil erosion and agricultural sustainability: *Proceedings of the National Academy of Sciences of the United States of America*, v. 104, no. 33, p. 13268-13272.
- Montgomery, D. R., and Brandon, M. T., 2002, Topographic controls on erosion rates in tectonically active mountain ranges: *Earth and Planetary Science Letters*, v. 201, no. 3, p. 481-489.
- Morris, G. L., and Fan, J., 1998, *Reservoir Sedimentation Handbook: Design and Management of Dams, Reservoirs and Watersheds for Sustainable Use*, McGraw-Hill, 848 p.
- Overstreet, W. C., White, A. M., Whitlow, J. W., Theobald Jr., P. K., Caldwell, D. W., Cuppels, N. P., and Stone, J., 1968, Fluvial monazite deposits in the southeastern United States, with a section on mineral analyses: *USGS Professional Paper no. 568*, 85 p.
- Parsons, A. J., Wainwright, J., Brazier, R. E., and Powell, D. M., 2006, Is sediment delivery a fallacy?: *Earth Surface Processes and Landforms*, v. 31, p. 1325-1328.
- Portenga, E. W., 2011, Using ^{10}Be to constrain erosion rates of bedrock outcrops globally and in the Central Appalachian Mountains: M.S. thesis, University of Vermont, Burlington, VT.
- Reiners, P. W., 2005, *Zircon (U-Th)/He Thermochronometry: Reviews in Mineralogy and Geochemistry*, v. 58, no. 1, p. 151-179.
- Reiners, P. W., and Brandon, M. T., 2006, Using Thermochronology to Understand Orogenic Erosion: *Annual Review of Earth and Planetary Sciences*, v. 34, no. 1, p. 419-466.
- Reusser, L., P. Bierman, and Rood, D., 2015, Quantifying human impacts on rates of erosion and sediment transport at a landscape scale: *Geology*, v. 43, no. 2, p. 171-174.
- Reuter, J., 2005, Erosion rates and patterns inferred from cosmogenic ^{10}Be in the Susquehanna River Basin: M.S. thesis, University of Vermont, Burlington, VT.
- Sadler, P. M., 1981, Sediment accumulation rates and the completeness of stratigraphic sections: *Journal of Geology*, v. 89, no. 5, p. 569-584.

- Sadler, P. M. and Jerolmack, D. J., 2014, Scaling laws for aggradation, denudation and progradation rates: the case for time-scale invariance at sediment sources and sinks, in Smith, D. G., R. J. Bailey, P. M. Burgess, and A. J. Fraser (eds.), *Strata and Time: Probing the Gaps in Our Understanding*, Geological Society, London, Special Publications, v. 404, p. 69-88.
- Schaller, M., von Blanckenburg, F., Hovius, N., and Kubik, P. W., 2001, Large-scale erosion rates from in situ-produced cosmogenic nuclides in European river sediments: *Earth and Planetary Science Letters*, v. 188, no. 3-4, p. 441-458.
- Snyder, N. P., Rubin, D. M., Alpers, C. N., Childs, J. R., Curtis, J. A., Flint, L. E., and Wright, S. A., 2004, Estimating accumulation rates and physical properties of sediment behind a dam: Englebright Lake, Yuba River, northern California: *Water Resources Research*, v. 40, no. 11, p. 1-19.
- Snyder, N. P., Nesheim, A. O., Wilkins, B. C., and Edmonds, D. A., 2013, Predicting grain size in gravel-bedded rivers using digital elevation models: Application to three Maine watersheds: *Geological Society of America Bulletin*, v. 125, no. 1-2, p. 148-163.
- Snyder, N. P., Merritts, D. J., Walter, R. C., Ames, E., Coplan, D., Dow, S., Johnson, K., Lewis, L., Meissner, J., Rahnis, M., Snyder-Fair, A., Wagner, D., and Waltner, M., 2017, How much anthropogenic soil erosion is stored in valley bottoms of the northeastern U.S.? Abstract EP31A-1845 presented at 2017 Fall Meeting, AGU, New Orleans, LA, 11-15 Dec.
- Summerfield, M. A., and Hulton, N. J., 1994, Natural controls of fluvial denudation rates in major world drainage basins: *Journal of Geophysical Research*, v. 99, no. B7, p. 13871-13883.
- Syvitski, J. P. M., and Milliman, J. D., 2007, Geology, Geography, and Humans Battle for Dominance over the Delivery of Fluvial Sediment to the Coastal Ocean: *The Journal of Geology*, v. 115, no. 1, p. 1-19.
- Tardy, Y., N'Kounkou, R., and Probst, J., 1989, The global water cycle and continental erosion during Phanerozoic time (570 my): *American Journal of Science*, v. 289, no. 4, p. 455-483.
- Trimble, S. W., 1977, The fallacy of stream equilibrium in contemporary denudation studies: *American Journal of Science*, v. 277, p. 876-887.
- Trimble, S. W., 1981, Changes in sediment storage in the Coon Creek basin, Driftless Area, Wisconsin, 1853 to 1975, *Science*, v. 214, no. 4517, p. 181-183.
- Troeh, F. R., Hobbs, R. L., and Donahue, R., 1999, *Soil and water conservation: Upper Saddle River, New Jersey*, Prentice-Hall, 610 p.

- Verstraeten, G., and Poesen, J., 2000, Estimating trap efficiency of small reservoirs and ponds: methods and implications for the assessment of sediment yield: *Progress in Physical Geography*, v. 24, no. 2, p. 219-251.
- Verstraeten, G., and Poesen, J., 2001, Variability of dry sediment bulk density between and within retention ponds and its impact on the calculation of sediment yields: *Earth Surface Processes and Landforms*, v. 26, no. 4, p. 375-394.
- Wakatsuki, T., and Rasyidin, A., 1992, Rates of weathering and soil formation: *Geoderma*, v. 52, no. 3-4, p. 251-263.
- Walling, D. E., 1994, Measuring sediment yield from river basins: *Soil Erosion Research Methods*, CRC Press, Chapter 3, p. 39-82.
- Walling, D. E., 1999, Linking land use, erosion and sediment yields in river basins: *Hydrobiologia*, v. 410, p. 223-240.
- Walter, R. C. and D. J. Merritts, 2008, Natural streams and the legacy of water-powered mills, *Science*, v. 319, p. 299-304.
- Wilkinson, B. H. and B. J. McElroy, 2007, The impact of humans on continental erosion and sedimentation, *Geological Society of America Bulletin*, v. 119, no. 1-2, p. 140-156.
- Wilkinson, B. H., 2005, Humans as geologic agents: A deep-time perspective: *Geology*, v. 33, no. 3, p. 161-164.
- Winslow, D. M., Zeitler, P. K., Chamberlain, C. P., and Hollister, L. S., 1994, Direct evidence for a steep geotherm under conditions of rapid denudation, Western Himalaya, Pakistan: *Geology*, v. 22, no. 12, p. 1075-1078.
- Wolman, M. G. and A. P. Schick, 1967, Effects of Construction on Fluvial Sediment, Urban and Suburban Areas of Maryland: *Water Resources Research*, v. 3, no. 2, p. 451-464.

APPENDIX 1: Y_s , E , location, drainage area, and timescale data for all points.

SOURCE	STATE	FEATURE NAME	Y_s (t km ⁻² yr ⁻¹)	E (mm yr ⁻¹)	GLAC	Lat (deg)	Long (deg)	Area (km ²)	Timescale (yrs)
<i>STREAM GAUGING</i>									
Reuter, 2005	PA	Juniata River at Newport, PA	12.7	0.0047	NO	40.47833	-77.1294	8686.9	17.0
	PA	Sherman Creek at Shermans Dale, PA	18.2	0.0067	NO	40.32333	-77.1692	536.1	8.0
	PA	Raystown Branch Juniata River at Saxton, PA	100.1	0.0371	NO	40.21583	-78.2656	1958.0	5.0
	PA	Bixler Run near Loysville, PA	25.7	0.0095	NO	40.37083	-77.4025	38.9	18.0
	PA	Swatara Creek at Harper Tavern, PA	119.2	0.0441	NO	40.4025	-76.5775	872.8	6.0
	PA	Little Conestoga Creek near Churchtown, PA	531.4	0.1968	NO	40.14472	-75.9889	15.1	10.0
	PA	Codorus Creek near York, PA	25.0	0.0092	NO	39.94611	-76.7556	575.0	5.0
	PA	Conestoga River at Conestoga, PA	67.2	0.0249	NO	39.94639	-76.3681	1217.3	15.0
	PA	Mill Creek at Eshelman Mill Road near Lyndon, PA	124.2	0.0460	NO	40.01	-76.2775	140.4	3.0
	PA	Susquehanna River at Towanda, PA	40.0	0.0148	YES	41.76528	-76.4411	20194.2	17.0
	NY	Chemung River at Chemung, NY	127.6	0.0473	YES	42.00222	-76.6347	6490.5	3.0
	PA	Tioga River at Tioga, PA	15.3	0.0057	YES	41.90833	-77.1297	730.4	6.0
	NY	Tioga River at Lindley, NY	155.5	0.0576	YES	42.02861	-77.1322	1996.9	7.0
	PA	Elk Run near Mainesburg, PA	62.5	0.0231	YES	41.815	-76.9653	26.4	13.0
PA	Corey Creek near Mainesburg, PA	42.9	0.0159	YES	41.79083	-77.015	31.6	15.0	
Conrad, 2000	NJ	Great Egg Harbor R Tr at Sicklerville	1.9	0.0007	NO	39.72528	-74.9608	147.9	5.0
	MD	Choptank R near Greensboro	6.2	0.0023	NO	38.99722	-75.7858	292.7	11.0
	MD	Susquehanna R at Conowingo	8.3	0.0031	NO	39.65778	-76.1744	70189.0	6.0
	NJ	Delaware R at Dunfield	12.8	0.0047	NO	40.97778	-75.1361	16389.5	10.0
	NJ	Baldwins C at Baldwin Lake near Pennington	16.0	0.0059	NO	40.34056	-74.78		7.0
	MD	NB Rock C near Rockville	16.8	0.0062	NO	39.1025	-77.12	161.1	10.0
	MD	Patuxent R near Bowie	21.9	0.0081	NO	38.95583	-76.6936	901.3	6.0
	NJ	Passaic R near Chatham	22.2	0.0082	NO	40.72528	-74.3897	1973.6	5.0
PA	Corey Creek near Mainesburg	35.7	0.0132	NO	41.79083	-77.015	31.6	11.0	

	NY	Mohawk R at Cohoes	43.8	0.0162	NO	42.78528	-73.7081		5.0
	PA	Steam Valley Run at Buttonwood	45.9	0.0170	NO	41.49417	-77.1508		5.0
	MD	Conococheague Creek at Fairview	46.8	0.0173	NO	39.71583	-77.8244	1279.5	13.0
	PA	Elk Run near Mainesburg	47.2	0.0175	NO	41.815	-76.9653		13.0
	MD	Monocacy R at Jug Bridge near Frederick	50.8	0.0188	NO	39.38778	-77.38	2116.0	9.0
	PA	Monongahela R at Braddock	58.4	0.0216	NO	40.39111	-79.8583	13830.6	6.0
	MD	NB Potomac R near Cumberland	61.6	0.0228	NO	39.62194	-78.7733	1051.5	16.0
	PA	Conodoguinet C Trib 1 near Enola	62.6	0.0232	NO	40.29083	-76.9939		7.0
	PA	Brandywine C at Chadds Ford	63.4	0.0235	NO	39.86917	-75.5931	743.3	15.0
	DE	Brandywine C at Wilmington	67.9	0.0251	NO	39.76917	-75.5736	813.3	31.0
	PA	Stony Fork near Elliottsville	82.6	0.0306	NO	39.76889	-79.6094		8.0
	PA	Stony Fork near Farmington	89.7	0.0332	NO	39.78083	-79.5753		12.0
	PA	Blockhouse C near English Center	95.3	0.0353	NO	41.47361	-77.2311	97.6	5.0
	PA	Blockhouse C at Buttonwood	100.9	0.0374	NO	41.49528	-77.1506		5.0
	PA	Enlow Fork near West Finley	100.9	0.0374	NO	39.96833	-80.4481		5.0
	PA	Blockhouse C trib at Liberty	102.7	0.0380	NO	41.56778	-77.1017		5.0
	PA	Conodoguinet C trib 3 near Enola	143.6	0.0532	NO	40.30139	-76.9492		7.0
	MA	Merrimack R bl Concord R at Lowell	18.5	0.0069	YES	42.64583	-71.2989	12100.5	5.0
Conrad, 2000	NY, NJ	Hudson River	10.0	0.0038	YES	40.70389	-74.0261	36001.0	
	NY, PA,								
	MD	Susquehanna River	12.0	0.0045	NO	39.55167	-76.0792	70999.7	
	PA, NY	Allegheny River	23.0	0.0087	NO	40.44361	-80.0142	29000.2	
	NJ	Raritan River	23.0	0.0087	NO	40.49389	-74.2842	7000.8	
	NJ	Passaic River	26.0	0.0098	NO	40.71333	-74.1194	1999.5	
	NY, PA,								
	NJ, DE	Delaware River	19.0	0.0072	NO	39.2775	-75.3572	18000.5	
	PA, MD,								
	MV, VA	Potomac River	33.0	0.0125	NO	37.97	-76.3042	38000.5	
	NH, MA	Merrimack River	2.4	0.0009	YES	42.81722	-70.8103	12999.2	
	ME	Kennebec River	2.4	0.0009	YES	43.755	-69.7811	15001.3	
	ME	Penobscot River	2.8	0.0011	YES	44.46861	-68.795	21999.5	
	MA, CT	Connecticut River	2.8	0.0011	YES	41.27333	-72.3361	29000.2	

Williams and Reed,
1972

PA	Fishing Creek near Bloomsburg, PA	34.0	0.0129	NO	41.07806	-76.4314	709.7
	Susquehanna River at Danville, PA	49.0	0.0186	NO	40.95806	-76.6194	29059.8
	West Branch Susquehanna River at Bower, PA	42.0	0.0159	NO	40.89694	-78.6772	815.9
	Driftwood Branch Sinnemahoning Creek at Sterling Run, PA	23.1	0.0088	NO	41.41333	-78.1972	704.5
	Spring Creek near Axemann, PA	38.5	0.0146	NO	40.88972	-77.7944	225.8
	Bald Eagle Creek at Milesburg, PA	31.9	0.0121	NO	40.94306	-77.7867	686.4
	Bald Eagle Creek at Blanchard, PA	28.0	0.0106	NO	41.05167	-77.6047	878.0
	Marsh Creek at Blanchard, PA	31.9	0.0121	NO	41.05944	-77.6061	114.2
	Pine Creek at Cedar Run, PA	26.3	0.0100	NO	41.52167	-77.4478	1564.4
	West Branch Susquehanna River at Lewisburg, PA	27.0	0.0102	NO	40.96806	-76.8736	17733.7
	Penns Creek at Penns Creek, PA	26.6	0.0101	NO	40.86667	-77.0486	779.6
	East Mahantango Creek near Dalmatia, PA	98.1	0.0372	NO	40.61111	-76.9122	419.6
	Juniata River at Huntingdon, PA	21.7	0.0082	NO	40.48472	-78.0192	2113.4
	Dunning Creek at Belden, PA	20.3	0.0077	NO	40.07167	-78.4928	445.5
	Raystown Branch Juniata River at Saxton, PA	31.5	0.0119	NO	40.21583	-78.2656	1958.0
	Kishacoquillas Creek at Reedsville, PA	21.4	0.0081	NO	40.65472	-77.5833	424.8
	Juniata River at Newport, PA	27.7	0.0105	NO	40.47833	-77.1294	8686.9
	Bixler Run near Loysville, PA	23.5	0.0089	NO	40.37083	-77.4025	38.9
	Sherman Creek at Shermans Dale, PA	29.8	0.0113	NO	40.32333	-77.1692	
	Susquehanna River at Harrisburg, PA	38.5	0.0146	NO	40.25472	-76.8864	62419.0
	Yellow Breeches Creek near Camp Hill, PA	45.5	0.0172	NO	40.22472	-76.8983	559.4
	Swatara Creek at Harper Tavern, PA	77.1	0.0292	NO	40.4025	-76.5775	
	West Conewago Creek near Manchester, PA	77.1	0.0292	NO	40.08222	-76.7203	1320.9
	South Branch Codorus Creek near York, PA	122.6	0.0464	NO	39.94611	-76.7556	
	Conestoga Creek at Lancaster, PA	63.1	0.0239	NO	40.05	-76.2775	839.2
NY	Susquehanna River at Unadilla, NY	23.1	0.0087	YES	42.32139	-75.3167	2543.4
	Unadilla River at Rockdale, NY	14.0	0.0053	YES	42.37778	-75.4061	1346.8
	Susquehanna River at Conklin, NY	27.7	0.0104	YES	42.03528	-75.8031	5780.9
	Chenango River at Greene, NY	17.5	0.0066	YES	42.32444	-75.7714	1535.9
	Owego Creek near Owego, NY	24.5	0.0093	YES	42.12917	-76.2706	479.2

		Susquehanna River near Waverly, NY	52.5	0.0198	YES	41.98472	-76.5011	12362.1	
		Tioga River at Lindley, NY	42.0	0.0159	YES	42.02861	-77.1325		
		Canisteo River at West Cameron, NY	154.1	0.0582	YES	42.22222	-77.4178	880.6	
		Tioga River near Erwins, NY	66.6	0.0251	YES	42.12111	-77.1292	3566.4	
		Cohocton River near Campbell, NY	49.0	0.0185	YES	42.2525	-77.2167	1217.3	
		Chemung River at Chemung, NY	52.5	0.0198	YES	42.00222	-76.6347		
Nagle et al, 2007	NY	Fall Creek; data from Forest Home site	42.0	0.0158	YES	42.45333	-76.4728	326.3	2.0
		Fall Creek; data from Freeville site	23.0	0.0087	YES	42.51389	-76.3475		1.25
		Virgil Creek; data from Freeville site	57.0	0.0215	YES	42.505	-76.35	104.4	1.25
		Six Mile Creek (W.Y. avg 2000, 2001)	170.5	0.0643	YES	42.40306	-76.435	101.0	2.0
		Genesee at Mt Morris	204.0	0.0770	YES	42.76667	-77.8389	3688.2	2.0
		Oatka Creek at Warsaw	20.0	0.0075	YES	42.74417	-78.1375	101.3	2.0
		Oatka Creek at Garbutt	6.0	0.0023	YES	43.01	-77.7914	518.0	2.0
		Mill Creek (Dansville NY)	119.0	0.0449	YES	42.55417	-77.7006		2.0
		West Branch Delaware at Beerston	24.0	0.0091	YES	42.12861	-75.1611		10.0
		Towne Brooke (upper West Branch Delaware)	67.0	0.0253	YES	42.35972	-74.6572		1.0
		Genesee at Portageville NY	197.0	0.0743	YES	42.57028	-78.0422	2548.6	2.0
		Genesee at Rochester	66.0	0.0249	YES	43.14172	-77.6163	6407.7	2.0
		Canaseraga Creek above Dansville	91.0	0.0343	YES	42.53556	-77.7042	230.3	2.0
		Canaseraga Creek at Shaker crossing	81.0	0.0306	YES	42.73694	-77.8408	867.7	2.0
		Black Creek at Churchville	3.0	0.0011	YES	43.10056	-77.8822	336.7	2.0
		Stony Brook NY Canaseraga Basin	86.0	0.0325	YES	42.50111	-77.6789		2.0
		Canisteo River at West Cameron	158.0	0.0596	YES	42.22222	-77.4178	880.6	
		Genesee at Mt. Morris Reservoir	158.0	0.0596	YES	42.76667	-77.8389		
		Schoharie Reservoir	90.0	0.0340	YES	42.35583	-74.445	815.9	
Bent, 2000	MA	Housatonic River near Great Barrington, MA	25.7	0.0097	YES	42.23194	-73.3547	730.4	2.0
		Williams River near Great Barrington, MA	51.5	0.0194	YES	42.2275	-73.3625	111.9	2.0
		Green River near Great Barrington, MA	42.9	0.0162	YES	42.19194	-73.3911	132.1	2.0
		Schenob Brook at Sheffield, MA	34.3	0.0129	YES	42.11417	-73.3508	129.5	2.0
		Ironworks Brook at Sheffield, MA	497.4	0.1877	YES	42.10889	-73.335	29.0	2.0
		Housatonic River near Ashley Falls, MA	94.3	0.0356	YES	42.07472	-73.3342	1204.4	2.0

		Konkapot River at Ashley Falls, MA	960.5	0.3624	YES	42.05306	-73.3264	158.2	2.0
Morrison, 1998	CT	Salmon River	96.7	0.0365	YES	41.55222	-72.4497	259.0	4.0
		Coginchaug River	10.3	0.0039	YES	41.52023	-72.7065	77.2	4.0
Kulp, 1983	CT	Yantic River	19.3	0.0073	YES	41.55861	-72.1219	231.3	5.0
Wemple, 2007	VT	Ranch Brook	6.1	0.0023	YES	44.52583	-72.7769		2.0
		West Branch	16.3	0.0062	YES	44.5025	-72.7853		2.0
Judson and Ritter, 1964	CT	Scantic R., Broad Brook	28.6	0.0102	YES	41.915	-72.5561	253.8	5.0
Kulp, 1991	CT	Muddy Brook at Woodstock	8.3	0.0031	YES	41.96556	-71.9625	52.1	1.3
Mansue and Comings, 1974	NJ	Delaware River	36.4	0.0138	NO	40.23389	-74.7931	17560.2	23.0
	NJ	Crosswicks Creek	32.6	0.0123	NO	40.10917	-74.6353	216.5	7.0
	PA	Neshaminy Creek	94.6	0.0358	NO	40.17694	-74.9442	543.9	2.0
	PA	Poquessing Creek	350.3	0.1327	NO	40.05056	-74.9928	55.7	3.0
	NJ	McDonalds Branch	1.7	0.0007	NO	39.87139	-74.6497	6.0	3.0
	PA	Pennypack Creek	112.1	0.0425	NO	40.04472	-75.0203	129.0	3.0
	NJ	South Branch Pennsauken Creek	57.8	0.0219	NO	39.94056	-74.9978	23.7	2.0
	PA	Frankford Creek	52.5	0.0199	NO	40.00333	-75.0908	69.9	3.0
	NJ	Cooper River	27.3	0.0103	NO	39.91194	-75.025	45.1	4.0
	NJ	South Branch Big Timber Creek	12.6	0.0048	NO	39.80417	-75.0742	49.2	2.0
	PA	Schuylkill River	10.5	0.0040	NO	40.53861	-75.9842	919.5	24.0
	PA	Perkiomen Creek	73.6	0.0279	NO	40.22306	-75.4503	722.6	10.0
	PA	Wissahickon Creek	273.2	0.1035	NO	40.10361	-75.2319	105.7	6.0
	PA	Schuylkill River	49.0	0.0186	NO	39.94278	-75.2031	4902.9	18.0
	NJ	Mantua Creek	46.6	0.0176	NO	39.73639	-75.1142	37.3	2.0
	PA	Darby Creek	304.7	0.1154	NO	39.90528	-75.2558	96.9	3.0
	NJ	Raccoon Creek	73.6	0.0279	NO	39.72667	-75.2589	77.4	6.0
	DE	White Clay Creek	119.1	0.0451	NO	39.73722	-75.7728	172.8	2.0
	DE	Brandywine Creek	56.0	0.0212	NO	39.73417	-75.5272	813.3	25.0
	NJ	Maurice River	3.1	0.0012	NO	39.54667	-75.0736	292.7	3.0
Mansue and Anderson, 1974	NJ	Stony Brook at Glenmoore	59.2	0.0224	NO	40.36722	-74.7894	45.6	4.0

		Honey Branch near Rosedale	48.7	0.0184	NO	40.34139	-74.7442	10.4	4.0
		Stony Brook Tributary No. 3 near Hopewell	9.8	0.0037	NO	40.40472	-74.7986	6.7	3.0
		Baldwin Creek at Pennington	141.9	0.0537	NO	40.33861	-74.8	5.0	4.0
		Woodsville Brook at Woodsville	95.6	0.0362	NO	40.37778	-74.8275	4.8	3.0
Wolman and Schick, 1967	MD	Watts Branch, Rockville	180.7	0.0685	NO	38.90111	-76.9422	9.6	
		Northwest Branch Anacostia R. near Colesville	164.6	0.0624	NO	39.06556	-77.0294	55.2	
		Georges Creek at Frankin	72.5	0.0275	NO	39.49389	-79.0447	187.5	
		Gunpowder Falls, Prettyboy Reservoir, Hereford	189.5	0.0859	NO	39.61889	-76.6903	207.2	28.0
		Seneca Creek, Dawsonville	112.1	0.0425	NO	39.12806	-77.3358	261.6	
		Gunpowder Falls, Loch Raven Dam, Towson	205.9	0.0780	NO	39.43028	-76.5436	777.0	47.0
		Monocacy River, Frederick	114.5	0.0434	NO	39.40278	-77.3661	2116.0	
		Little Falls Branch, Bethesda	812.6	0.3078	NO	38.96	-77.1031	10.6	
		Northwest Branch Anacostia R. near Hyattsville	648.0	0.2455	NO	38.95222	-76.9661	127.9	
	Wash. DC	Rock Creek	560.4	0.2123	NO	38.9725	-77.04	161.1	
	MD	Northeast Branch Anacostia R. near Riverdale	371.3	0.1406	NO	38.96028	-76.9261	188.6	
Chin, 1986	MD	Kensington	9267.0	3.5102	NO	39.02417	-77.0708	0.24	
	MD	Little Patuxent at Guilford	236.0	0.0894	NO	39.16778	-76.8514	98.4	
	NJ	Delaware R. near Trenton	193.0	0.0731	NO	40.22167	-74.7781	17560	
	MD	NW Branch Anacostia R., Hyattsville	714.0	0.2705	NO	38.95222	-76.9661	128	
Wolman, 1967	MD	Broad Ford Run	3.9	0.0015	NO	39.39083	-79.3886	19.166	
		Fishing Creek	1.8	0.0007	NO	39.51889	-77.4539	18.907	
		Stony Run	18.9	0.0072	NO	39.17472	-76.6964	6.3973	

LAKE SEDIMENTATION									
Cook, 2015	VT	Amherst (Plymouth, VT)	21.4	0.0080	YES	43.48862	-72.7034	49.4	2030
	VT	Beebe (Hubbardton, VT)	29.5	0.0110	YES	43.73588	-73.1814	7.5	8590
	NY	Chapel (Saint Huberts, NY)	5.3	0.0020	YES	44.13916	-73.7464	4.6	11400
	VT	Duck (Sutton, VT)	26.2	0.0100	YES	44.68195	-72.0679	0.7	13000
	VT	Dunmore (Salisbury, VT)	64.3	0.0240	YES	43.90902	-73.0714	52.9	6250
	VT	Echo (Plymouth, VT)	14.1	0.0050	YES	43.47235	-72.6999	68.1	2050
	VT	Elligo (Greensboro, VT)	108.4	0.0400	YES	44.59425	-72.3554	13.1	3470

VT	Emerald (Dorset, VT)	6.9	0.0030	YES	43.27489	-73.0074	14.7	8500
VT	Morey (Fairlee, VT)	65.6	0.0240	YES	43.91907	-72.1573	20.7	12000
NY	Thirteenth (North River, NY)	48.7	0.0180	YES	43.70777	-74.1264	28.5	6810
VT	Vail (Sutton, VT)	21.2	0.0080	YES	44.70498	-72.0721	2	9380
NH	Crystal Lake (Eaton, NH)	17.1	0.0060	YES	43.91042	-71.0746	15	13350
NH	Ogontz Lake (Lyman, NH)	15.3	0.0060	YES	44.26536	-71.9061	23.6	4930
NH	Stinson Lake (Rumney, NH)	25.2	0.0090	YES	43.87	-71.8	20.7	14500
NH	South Pond (Stark, NH)	28.4	0.0110	YES	44.6	-71.37	7.4	11520
NH	Sandy Pond (Richmond, NH)	40.4	0.0150	YES	42.77	-72.45	1.1	13590
ME	Worthley Pond (Peru, ME)	39.0	0.0140	YES	44.4	-70.43	13.5	14460
VT	Richmond (Richmond, VT)	22.4	0.0080	YES	44.41777	-72.9471	2.2	8850
VT	Ritterbush (Eden, VT)	14.7	0.0050	YES	44.74637	-72.5993	2.2	9510
MA	Wicket Pond (Wendell, MA)	46.4	0.0170	YES	42.55118	-72.4319	0.952	2080
NH	Pecker Pond (Rindge, NH)	68.0	0.0250	YES	42.71476	-71.9635	0.786	1400
NH	North Round Pond	121.1	0.0450	YES	42.84784	-72.4517	0.213	1490
MA	Little Pond (Bolton, MA)	78.8	0.0290	YES	42.42234	-71.5877	0.32	3009
VT	Knob Hill Pond (Marshfield, VT)	84.0	0.0310	YES	44.3605	-72.3737	0.56	13814

RESERVOIR

SEDIMENTATION

McCusker and Daniels,
2008

CT	Willimantic River Dam	19.9	0.0075	YES	41.78472	-72.2808	288	148
	Schoolhouse Brook Dam	744.5	0.2809	YES	41.77889	-72.2242	2	34
	US Pomperaug Dam	0.6	0.0002	YES	41.5225	-73.2078	165	138
	DS Pomperaug Dam	0.03	0.00001	YES	41.52667	-73.2106	205	108
	Blackberry River Dam	0.1	0.0000	YES	42.01083	-73.2914	116	258

Ahamed, 2014

CT	BROAD BROOK	53.7	0.0203	YES	41.91726	-72.5457	13.3	35.2
MA	MOUNTAIN STREET	223.4	0.0843	YES	42.4001	-72.6707	2.1	46.2
CT	PLANTS POND	6.3	0.0024	YES	41.51	-72.2636	40.8	100.9
CT	SOUTHINGTON RESERVOIR	40.3	0.0152	YES	41.5765	-72.9344	2.8	68.2
CT	WALLINGFORD	16.9	0.0064	YES	41.4363	-72.7782	23.3	10.2
MA	WEST WHATELY	11.7	0.0044	YES	42.4415	-72.6854	23.3	49.2

MA	WESTFIELD	41.6	0.0157	YES	42.1904	-72.8115	6.5	77.2
NY	SCHOHARIE (GILBOA DAM)	69.8	0.0263	YES	40.3833	-74.4333	813.3	23.7
NJ	ENGLISHTOWN POND	9.5	0.0036	YES	40.2917	-74.3561	18.6	200.3
NJ	CARNEGIE LAKE	25.9	0.0098	YES	40.3350	-74.6519	401.4	51.6
NY	WAPPINGER	6.3	0.0024	YES	41.6008	-73.9197	510.2	52.0
NY	BATAVIA KILL, SITE NO. 4A	12.5	0.0047	YES	42.3333	-74.2500	17.6	7.0
MD	LOCH RAVEN RESERVOIR	247.6	0.0934	NO	39.4306	-76.5450	784.8	58.3
MD	PRETTYBOY	225.0	0.0849	NO	39.6195	-76.7073	207.2	28.4
PA	GRIFFIN	98.3	0.0371	YES	41.4969	-75.6647	8.3	52.9
PA	ELMHURST	15.6	0.0059	YES	41.3708	-75.5388	90.3	50.9
PA	LAKE WILLIAMS	191.0	0.0721	NO	39.8917	-76.7290	111.1	26.8
PA	WILLIAMS BRIDGE	10.4	0.0039	YES	41.3822	-75.6234	12.9	47.9
MD	ATKISSON RESERVOIR	122.9	0.0464	NO	39.4765	-76.3389	117.7	23.0
NY	PELTO DAM	41.9	0.0158	YES	42.2167	-76.5333	1.1	10.7
NY	PYLKAS DAM	34.9	0.0132	YES	42.1667	-76.5167	1.8	13.7
NJ	COLUMBIA DAM	8.7	0.0033	YES	40.9239	-75.0873	442.9	20.0
PA	OLD GLATFELTER RESERVOIR	16.1	0.0061	NO	39.8080	-76.8836	192.4	54.8
NY	LAKE RUSHFORD	163.7	0.0618	YES	42.3804	-78.1831	157.2	26.3
PA	ICEDALE	8.4	0.0032	NO	40.0701	-75.8367	51.8	51.0
PA	COATSVILLE RESERVOIR	114.8	0.0433	NO	40.0053	-75.8531	12.9	35.0
MD	LIBERTY RESERVOIR	189.4	0.0715	NO	39.3667	-76.8333	424.8	7.9
MD	LITTLE DEER CREEK NO. 1	518.0	0.1955	NO	39.6436	-76.5008	1.9	13.8
NY	MOUNT MORRIS	103.7	0.0391	YES	42.7329	-77.9072	2789.4	11.4
NY	PATTERSON CREEK, SITE NO. 1	68.0	0.0257	YES	42.1333	-76.0167	11.1	9.0
NY	LITTLE CHOCONUT, SITE NO. 2B	45.4	0.0171	YES	42.1833	-75.9667	4.2	9.0
PA	EAST BRANCH CLARION RIVER LAKE	287.1	0.1083	NO	41.5600	-78.5933	187.5	18.9
PA	KAERCHER CREEK, PA-476	91.1	0.0344	NO	40.5694	-75.8458	1.3	9.7
PA	MARTIN CREEK, PA-467	45.4	0.0171	YES	41.7667	-75.7500	2.1	8.0
PA	MARSH CREEK, PA-600	727.3	0.2744	YES	41.7500	-77.5000	8.1	10.9
PA	GREENE-DREHER, PA-446	17.2	0.0065	YES	41.2333	-75.3333	12.4	12.9
PA	LITTLE SCHUYLKILL WATERSHED	37.3	0.0141	NO	40.6933	-75.9442	2.8	13.9

NY	NEWTON-HOFFMAN SITE 1	28.4	0.0107	YES	42.1739	-76.6658	9.0	2.8
MD	BURNT MILLS	59.2	0.0708	NO	39.0308	-77.0065	69.9	7.8
MD	GREENBELT LAKE	187.6	0.3906	NO	39.0021	-76.8908	2.1	31.9
MD	TRIADELPHIA LAKE (BRIGHTON DAM)	309.6	0.1168	NO	39.2000	-77.0000	210.8	22.1
PA	GORDON LAKE	378.3	0.1427	NO	39.7476	-78.6761	165.8	26.6
PA	THOMAS W. KOON LAKE	22.7	0.0085	NO	39.7640	-78.6643	155.4	8.1
MD	SAVAGE RIVER DAM	292.3	0.1103	NO	39.5077	-79.1328	271.9	4.0
MD	ROCKY GORGE	494.3	0.1865	NO	39.1167	-76.8833	344.0	10.4
MD	WILDE LAKE	3336.7	1.2591	NO	39.2236	-76.8592	4.9	2.9
PA	HINCKSTON RUN RESERVOIR	181.1	0.0683	NO	40.3737	-78.8862	27.8	32.3
PA	QUEMAHONING	165.0	0.0623	NO	40.1821	-78.9428	238.3	25.7
PA	SALT LICK RESERVOIR	100.9	0.0381	NO	40.3817	-78.8334	30.7	23.3
PA	TIONESTA LAKE	32.6	0.0123	NO	41.4767	-79.4467	1238.0	30.3
PA	LOYALHANNA	143.2	0.0540	NO	40.4569	-79.4514	751.1	19.8
PA	MAHONING CREEK	78.3	0.0296	NO	40.9218	-79.2780	880.6	24.0
PA	CROOKED CREEK	104.9	0.0396	NO	40.7146	-79.5100	717.4	24.3
PA	YOUGHIOGHENY RIVER LAKE	215.1	0.0812	NO	39.7989	-79.3683	1124.1	30.0
MD	MOUNTAIN LAKE	37.4	0.0141	NO	39.4079	-79.3712	19.2	77.1
NY	ORCHARD PARK	71.2	0.0269	YES	42.6901	-78.6533	4.3	23.3
NY	ISCHUA CREEK, SITE NO. 2	12.8	0.0048	YES	42.3833	-78.4167	7.3	10.2
NY	ISCHUA CREEK, SITE NO. 5	19.4	0.0073	YES	42.3167	-78.4167	16.6	10.2
PA	NORTH FORK COWANESQUE RIVER	23.1	0.0087	YES	41.9956	-77.6494	8.8	14.9
NY	CONEWANGO CREEK SITE 9A	53.4	0.0201	YES	42.3847	-79.1161	15.5	3.9

**COSMOGENIC
NUCLIDES**

Reuter, 2005	PA	Kyler Fork of Yost Run	17.6	0.0066	NO	41.16354	-77.9048	0.583	249000
		Pebble Run	29.4	0.0111	NO	41.24449	-78.2781	6.444	149000
		Wykoff Branch--HIGH--LOCATION UNCERTAIN	23.7	0.0090	NO	41.45243	-77.976	1.245	184000
		Big Run	49.0	0.0185	NO	41.45871	-78.4299	3.153	89200
		trib to Little Birch Island Run	32.8	0.0124	NO	41.2045	-78.0339	3.368	134000
		Little Birch Island Run	33.6	0.0127	NO	41.20353	-78.0387	6.471	130000

Middle Branch	26.4	0.0099	NO	41.20309	-77.7976	3.068	166000
Sanders Draft	38.5	0.0145	NO	41.27551	-78.2334	4.829	114000
Wykoff Branch--LOW	36.8	0.0139	NO	41.45135	-77.9522	4.676	119000
Bell Draft	38.7	0.0146	NO	41.39568	-78.3569	5.384	113000
Heth Run--LOCATION UNCERTAIN	82.4	0.0311	NO	41.70411	-78.0375	3.532	53000
Lebo Branch	49.2	0.0186	NO	41.35824	-77.9689	3.885	89000
Yost Run--LOW	54.6	0.0206	NO	41.20881	-77.9214	15.121	80000
East Branch	58.6	0.0221	NO	41.44815	-78.3593	3.194	75000
another Middle Branch	91.9	0.0347	NO	41.42724	-78.3592	3.384	48000
Drake Hollow	55.3	0.0209	NO	41.28568	-77.7894	4.018	79000
Left Fork Bearfield Run	100.5	0.0379	NO	41.38583	-77.9492	3.445	43000
Crooked Run	86.7	0.0327	NO	41.59207	-78.1866	5.596	50000
Laurely Fork	88.0	0.0332	NO	41.27427	-77.7678	5.312	50000
South Branch Little Portage Creek	104.6	0.0395	NO	41.59802	-78.1037	3.151	42000
Dry Run	66.9	0.0252	NO	41.37575	-78.1535	2.959	65000
Russell Hollow Run	142.1	0.0536	NO	41.45843	-78.1529	3.193	31000
Gottshall Run--LOW	62.1	0.0234	NO	41.09765	-77.2461	9.699	70000
Gottshall Run--HIGH	45.1	0.0170	NO	41.08517	-77.2746	2.12	97000
Jamison Run	23.9	0.0090	NO	41.06914	-77.3078	5.531	183000
trib to White Deer Hole Run	36.9	0.0139	NO	41.0747	-77.1189	3.18	119000
Buffalo Creek	17.5	0.0066	NO	40.94032	-77.2228	3.135	249000
Wolf Run	22.6	0.0085	NO	40.52224	-76.7463	2.989	193000
Minehart Run	29.9	0.0113	NO	40.53022	-77.6098	8.647	146000
trib to Minehart Run	39.1	0.0147	NO	40.53099	-77.6091	3.783	112000
Wharton Run	61.1	0.0230	NO	40.40713	-77.7673	3.155	72000
Shores Branch	19.6	0.0074	NO	40.32638	-78.0484	3.099	223000
Laurel Run	25.7	0.0097	NO	40.33224	-78.1113	4.49	170000
Croyle Run	14.3	0.0054	NO	40.69622	-77.8027	3.024	305000
another Laurel Run	18.8	0.0071	NO	40.73779	-77.7901	3.15	232000
Swift Run	45.3	0.0171	NO	40.81642	-77.4179	3.261	96000
Pine Swamp Run	37.9	0.0143	NO	40.83199	-77.4763	3.298	115000

Bear Run	76.5	0.0289	NO	40.98545	-77.4854	3.218	57000
trib from Kettle Mountain	54.8	0.0207	NO	40.98213	-77.4903	4.847	80000
Sulphur Run	26.3	0.0099	NO	41.2055	-77.3404	2.675	166000
Mud Creek	30.3	0.0114	NO	41.07412	-76.6177	6.361	144000
trib to Spruce Run Creek	40.5	0.0153	NO	41.0754	-76.5221	5.195	108000
trib to Plum Creek	17.5	0.0066	NO	40.85166	-76.7164	3.789	250000
Independence Run	41.3	0.0156	NO	40.68602	-76.8977	5.612	106000
Boyers Run	49.5	0.0187	NO	40.62494	-76.9564	3.961	88000
trib to Lick Run	10.3	0.0039	NO	40.36875	-77.6557	3.292	424000
trib to Frankstown Branch Juniata River	24.7	0.0093	NO	40.44251	-78.3026	2.807	177000
Greens Run	54.3	0.0205	NO	41.01479	-77.7065	3.041	81000
Anderson Run	23.7	0.0090	NO	39.81207	-76.33	3.936	184000
Mill Creek--HIGH	14.8	0.0056	NO	39.81509	-76.3463	3.041	296000
trib to Conowingo Creek	30.4	0.0115	NO	39.82879	-76.1884	25.297	144000
Kellys Run	22.3	0.0084	NO	39.83688	-76.339	5.441	196000
trib to Tucquan Creek	23.1	0.0087	NO	39.86501	-76.3402	4.09	190000
trib to Beaver Creek	25.8	0.0097	NO	39.90078	-76.5199	4.407	169000
trib to Bald Eagle Creek	32.3	0.0122	NO	39.74955	-76.4353	3.926	135000
Alum Rock Run	24.4	0.0092	NO	39.77574	-76.4934	7.005	180000
another trib to East Branch	22.7	0.0086	NO	39.80579	-76.6202	7.469	193000
trib to East Branch	25.6	0.0097	NO	39.81624	-76.6498	3.805	171000
Green Branch	22.4	0.0084	NO	39.9358	-76.4735	3.379	195000
Driftwood Br Sinnemahoning Cr at Sterling Run, PA	57.2	0.0216	NO	41.41333	-78.1972	705.04	76000
West Branch Susquehanna River at Bower, PA	51.4	0.0194	NO	40.89694	-78.6772	815.81	85000
Juniata River at Newport, PA	50.2	0.0189	NO	40.47833	-77.1294	8685.9	87000
Sherman Creek at Shermans Dale, PA	29.4	0.0111	NO	40.32333	-77.1692	534.98	149000
Raystown Branch Juniata River at Saxton, PA	24.7	0.0093	NO	40.21583	-78.2656	1955.2	177000
Dunning Creek at Belden, PA	24.1	0.0091	NO	40.07167	-78.4928	445.22	181000
Bald Eagle Creek bl Spring Creek at Milesburg, PA	43.5	0.0164	NO	40.94306	-77.7867	690.09	100000
Bixler Run near Loysville, PA	20.4	0.0077	NO	40.37083	-77.4025	38.819	214000
Spring Creek near Axemann, PA	35.2	0.0133	NO	40.88972	-77.7944	224.33	124000

		Yellow Breeches Creek near Camp Hill, PA	50.7	0.0191	NO	40.22472	-76.8983	558.49	86000
		Swatara Creek at Harper Tavern, PA	36.3	0.0137	NO	40.4025	-76.5775	870.2	120000
		West Conewago Creek near Manchester, PA	37.4	0.0141	NO	40.08222	-76.7203	1326.2	117000
		Little Conestoga Creek near Churchtown, PA	25.6	0.0097	NO	40.14472	-75.9889	15.092	171000
		Codorus Creek near York, PA	35.9	0.0135	NO	39.94611	-76.7556	573.38	122000
		Pequea Creek at Martic Forge, PA	51.5	0.0194	NO	39.90583	-76.3286	381.82	85000
		Conestoga River at Conestoga, PA	48.2	0.0182	NO	39.94639	-76.3681	1211.8	91000
		Mill Creek at Eshelman Mill Road near Lyndon, PA	29.1	0.0110	NO	40.01	-76.2775	140.67	150000
		Little Conestoga Creek near Millersville, PA	25.5	0.0096	NO	40.02083	-76.3592	104.62	171000
Del Vecchio et al., 2017 (in prep)	PA	Garners Run stream sediment, Shale Hills CZO	17.5	0.0066	NO	40.680	-77.951		
		GR2	14.1	0.0053	NO	40.679	-77.955		
THERMOCHRONOLOGY									
Roden and Miller, 1989	PA	Dubois	69.5	0.0262	NO	41.11861	-78.7603		1.41E+08
		Johnstown	156.3	0.0590	NO	40.32694	-78.9244		7.80E+07
		Hyndman	65.3	0.0246	NO	39.81917	-78.7211		2.03E+08
		Grazierville	56.9	0.0215	NO	40.65417	-78.2642		2.33E+08
		Bald Hill	53.9	0.0203	NO	40.42278	-78.3408		2.46E+08
		Altoona	301.0	0.1136	NO	40.50333	-78.4006		4.40E+07
		I-80	98.1	0.0370	NO	40.94944	-77.7428		1.35E+08
		Lock Haven	163.9	0.0619	NO	41.06167	-77.4628		9.70E+07
		Dickey's Mt	86.4	0.0326	NO	39.73222	-78.1747		2.33E+08
		Orbisonia	93.7	0.0353	NO	40.21333	-77.8997		2.15E+08
		Entriiken	84.1	0.0317	NO	40.28028	-78.1997		1.89E+08
		Mapleton	71.0	0.0268	NO	40.35972	-77.9442		2.24E+08
		Newton-Hamilton	89.5	0.0338	NO	40.37472	-77.8381		2.25E+08
		Old Port	82.2	0.0310	NO	40.50833	-77.3914		2.45E+08
		Powys	123.0	0.0464	YES	41.295	-77.0975		1.40E+08
		Falls Creek	132.5	0.0500	YES	41.625	-76.6322		1.52E+08
		Wyalusing	136.8	0.0516	YES	41.59611	-76.2647		1.55E+08

		Selinsgrove	103.3	0.0390	NO	40.74361	-76.8597	2.18E+08
		Wardville	120.5	0.0455	NO	40.59583	-77.0033	1.87E+08
		Midway	109.9	0.0415	NO	40.43889	-76.9214	2.05E+08
		Swatara Gap	156.9	0.0592	NO	40.43472	-76.5264	1.52E+08
		Pittston	201.5	0.0760	YES	41.32333	-75.7906	1.21E+08
		Falls	172.9	0.0652	YES	41.44944	-75.8472	1.41E+08
		Avoca	192.0	0.0724	YES	41.3325	-75.7081	1.27E+08
		Bartonsville	132.5	0.0500	YES	41.02972	-75.3056	1.84E+08
		Kittatinny Mt.	169.3	0.0639	YES	40.92972	-75.1831	1.44E+08
		Stroudsburg	137.7	0.0520	YES	40.98056	-75.1944	1.77E+08
Roden-Tice et al., 2009	NH	Southern	82.9	0.0313	YES	42.834	-72.358	1.28E+08
			110.4	0.0417	YES	42.792	-72.455	9.60E+07
			90.1	0.0340	YES	42.923	-72.455	1.18E+08
			93.3	0.0352	YES	43.179	-71.688	1.14E+08
			92.8	0.0350	YES	43.436	-72.043	1.14E+08
			89.8	0.0339	YES	43.239	-71.459	1.18E+08
			88.0	0.0332	YES	43.238	-71.57	1.20E+08
			83.3	0.0314	YES	43.269	-71.459	1.27E+08
			112.5	0.0425	YES	43.425	-71.26	9.42E+07
			129.1	0.0487	YES	43.298	-72.195	8.21E+07
			105.8	0.0399	YES	42.987	-72.382	1.00E+08
			84.1	0.0317	YES	42.913	-72.12	1.26E+08
			95.9	0.0362	YES	42.907	-72.075	1.11E+08
			88.0	0.0332	YES	42.887	-71.999	1.20E+08
			103.1	0.0389	YES	43.179	-71.821	1.03E+08
			101.8	0.0384	YES	43.238	-71.916	1.04E+08
			126.2	0.0476	YES	43.359	-72.192	8.40E+07
	ME	Western	103.9	0.0392	YES	43.954	-70.898	1.02E+08
			97.3	0.0367	YES	44.244	-70.883	1.09E+08
			91.1	0.0344	YES	44.338	-70.669	1.16E+08
			131.8	0.0498	YES	44.653	-70.708	8.04E+07

		110.9	0.0418	YES	44.384	-70.652	9.56E+07
		99.3	0.0375	YES	44.4	-70.804	1.07E+08
		108.4	0.0409	YES	44.371	-70.631	9.78E+07
		112.5	0.0425	YES	44.807	-70.672	9.42E+07
		94.0	0.0355	YES	43.74	-70.782	1.13E+08
		106.9	0.0403	YES	43.456	-70.911	9.92E+07
VT	Northeastern	130.2	0.0491	YES	44.707	-71.874	8.14E+07
		117.8	0.0444	YES	44.828	-71.964	9.00E+07
		90.0	0.0340	YES	44.91	-72.007	1.18E+08
		129.3	0.0488	YES	44.941	-71.853	8.20E+07
NH	Northern	99.6	0.0376	YES	44.851	-71.552	1.06E+08
		90.4	0.0341	YES	44.865	-71.312	1.17E+08
		113.0	0.0426	YES	44.858	-71.286	9.38E+07
		114.7	0.0433	YES	44.812	-71.244	9.24E+07
NH	Northwestern	81.5	0.0308	YES	44.471	-71.546	1.30E+08
		84.8	0.0320	YES	44.687	-71.589	1.25E+08
		83.0	0.0313	YES	44.26	-71.829	1.28E+08
		76.1	0.0287	YES	44.109	-72.039	1.39E+08
		81.3	0.0307	YES	44.316	-71.826	1.30E+08
		75.7	0.0286	YES	44.244	-71.874	1.40E+08
VT	Ammonoosuc Fault	86.0	0.0324	YES	43.909	-72.142	1.23E+08
		91.3	0.0345	YES	43.825	-72.332	1.16E+08
		87.9	0.0332	YES	43.696	-72.403	1.21E+08
NH	Ammonoosuc Fault	99.8	0.0377	YES	43.156	-72.447	1.06E+08
		106.0	0.0400	YES	43.662	-72.254	1.00E+08
		102.1	0.0385	YES	43.683	-72.269	1.04E+08
		106.1	0.0400	YES	43.177	-72.43	9.99E+07
		109.6	0.0414	YES	43.159	-72.376	6.70E+06
		101.4	0.0383	YES	43.186	-72.294	1.05E+08
NH	White Mountains	134.5	0.0508	YES	43.902	-71.993	7.88E+07
		127.1	0.0480	YES	43.842	-71.905	8.34E+07

			150.8	0.0569	YES	43.567	-72.158	7.03E+07
			107.6	0.0406	YES	44.589	-71.193	9.85E+07
			124.9	0.0471	YES	44.445	-71.191	8.49E+07
			124.3	0.0469	YES	44.367	-71.308	8.53E+07
			112.6	0.0425	YES	43.632	-71.993	9.41E+07
			109.1	0.0412	YES	43.559	-71.943	9.72E+07
			114.3	0.0431	YES	43.939	-71.874	9.27E+07
			123.5	0.0466	YES	43.973	-71.79	8.58E+07
			117.9	0.0445	YES	44.034	-71.772	8.99E+07
			122.3	0.0461	YES	44.179	-71.692	8.67E+07
			122.3	0.0461	YES	44.253	-71.447	8.67E+07
			123.0	0.0464	YES	44.047	-71.294	8.62E+07
			124.3	0.0469	YES	43.857	-71.652	8.53E+07
	NH	Ossipee Mtn Complex	112.2	0.0423	YES	43.817	-71.297	9.45E+07
Blackmer et al., 1994	PA	PA-17	49.7	0.0188	NO	39.85028	-80.395	1.44E+08
		PM-2	42.8	0.0162	NO	39.88167	-80.3969	1.67E+08
		PM-1	41.6	0.0157	NO	40.07222	-80.2286	1.72E+08
		PMN-1	50.4	0.0190	NO	39.8675	-79.9794	1.42E+08
		PA-9	38.9	0.0147	NO	40.70139	-79.7	1.84E+08
		PG-1	50.7	0.0191	NO	40.56194	-79.2192	1.41E+08
		PA-13	54.6	0.0206	NO	40.83694	-78.6581	1.31E+08
		CK-8	46.5	0.0175	NO	41.23833	-78.2858	1.54E+08
		CK-7	59.7	0.0225	NO	39.85028	-79.4894	1.51E+08
		PA-15	58.9	0.0222	NO	40.03806	-79.2086	1.53E+08
		PA-3	67.7	0.0256	NO	40.285	-78.8722	1.33E+08
		PA-2	64.8	0.0245	NO	40.52278	-78.5547	1.39E+08
		D-3	65.8	0.0248	NO	40.51917	-78.4092	1.37E+08
		CK-1	60.9	0.0230	NO	41.26417	-77.7961	1.48E+08
		CK-9	54.0	0.0204	NO	41.15944	-77.4789	1.67E+08
		CK-10	58.1	0.0219	YES	41.46556	-77.3208	1.55E+08
		CK-11	67.2	0.0254	YES	41.46833	-76.6792	1.34E+08

		CK-3	86.9	0.0328	NO	40.25528	-78.0592	1.25E+08
		J-1	76.5	0.0289	NO	40.95889	-77.5314	1.42E+08
		BE-7	70.1	0.0265	NO	41.03694	-77.3089	1.55E+08
		BE-11	66.7	0.0252	NO	41.12028	-77.1936	1.63E+08
		BE-10	74.4	0.0281	?	41.15917	-77.0669	1.46E+08
		D-4	66.3	0.0250	NO	40.48611	-77.1675	1.64E+08
		PL-6	150.4	0.0567	NO	40.76833	-76.4333	1.41E+08
		D-5	172.4	0.0650	YES	41.10944	-76.3681	1.23E+08
		PL-1	147.2	0.0556	YES	41.21611	-76.0922	1.44E+08
		D-7	191.0	0.0721	YES	41.36111	-75.6242	1.11E+08
		PL-2	151.4	0.0571	YES	41.44222	-75.7436	1.40E+08
		CK-12	158.2	0.0597	YES	41.47111	-75.8436	1.34E+08
Kunk et al., 2005	MD	Potomac Terrane	116.5	0.0440	NO	38.9818	-77.2402	4.55E+08
			92.8	0.0350	NO	38.918	-77.2383	4.17E+08
			111.6	0.0421	NO	38.963	-77.2372	4.75E+08
			103.2	0.0389	NO	38.9762	-77.2139	3.75E+08
			109.3	0.0412	NO	38.9763	-77.1738	3.54E+08
			130.9	0.0494	NO	38.9718	-77.1383	4.05E+08
			110.5	0.0417	NO	38.9593	-77.1074	3.50E+08
			131.2	0.0495	NO	38.9267	-77.044	4.04E+08
			133.2	0.0503	NO	38.9268	-77.0439	3.98E+08
Roden-Tice et al., 2000	NY	Mount Marcy	63.1	0.0240	YES	44.12	-73.92	1.68E+08
		Dix	65.8	0.0250	YES	44.08	-73.79	1.61E+08
		Blue Mountain Lake	72.6	0.0270	YES	43.87	-74.43	1.46E+08
		Whiteface	74.8	0.0280	YES	44.37	-73.87	1.42E+08
		Van der Wacker	71.5	0.0270	YES	43.9	-74.09	1.48E+08
		Hurricane	71.0	0.0270	YES	44.24	-73.7	1.49E+08
		Saranac Lake	66.9	0.0250	YES	44.27	-74.36	1.59E+08
		Giant	78.8	0.0300	YES	44.16	-73.7	1.35E+08
		North Fork Boquet	99.3	0.0370	YES	44.11	-73.69	1.07E+08
		Lyon Mountain	76.4	0.0290	YES	44.71	-73.87	1.39E+08

Terry Mountain	72.8	0.0270	YES	44.57	-73.63	1.46E+08
Vermontville	92.8	0.0350	YES	44.55	-74.05	1.14E+08
Alder Brook	86.7	0.0330	YES	44.45	-74.07	1.22E+08
Altona Flatrock (ss)	85.1	0.0320	YES	44.86	-73.67	1.25E+08
Chateaguay (ss)	74.0	0.0280	YES	43.93	-75.38	1.43E+08
Kents Corners	80.6	0.0300	YES	44.44	-75.3	1.32E+08
Clifton	83.9	0.0320	YES	44.23	-74.78	1.26E+08
Fine	78.4	0.0300	YES	44.25	-75.14	1.35E+08
Port Leyden	78.0	0.0290	YES	43.59	-75.84	1.36E+08
Brantingham Lake	75.3	0.0280	YES	43.69	-75.3	1.41E+08
Hinckley Reservoir	84.7	0.0320	YES	43.36	-75.04	1.25E+08
Old Forge	74.1	0.0280	YES	43.71	-74.97	1.43E+08
Little Falls	81.5	0.0310	YES	43.04	-74.86	1.30E+08
Lake Pleasant	76.4	0.0290	YES	43.48	-74.4	1.39E+08
Gilmantown	78.4	0.0300	YES	43.43	-74.31	1.35E+08
Moose Mountain	81.0	0.0310	YES	43.5	-74.31	1.31E+08
North Creek	80.0	0.0300	YES	43.68	-73.99	1.33E+08
Minerva	86.2	0.0330	YES	43.81	-74.01	1.23E+08
Baker Brook	94.3	0.0360	YES	43.6	-74.06	1.12E+08
Johnsburg	101.8	0.0380	YES	43.62	-73.96	1.04E+08
Pharaoh Mountain	107.6	0.0410	YES	43.82	-73.65	9.85E+07
Crane Mountain	110.3	0.0420	YES	43.54	-73.65	9.61E+07
Fort Ann (ss)	115.3	0.0440	YES	43.41	-73.52	9.19E+07
Lake George	112.9	0.0430	YES	43.4	-73.71	9.39E+07
Ticonderoga	128.2	0.0480	YES	43.85	-73.59	8.27E+07
Schroon Lake	101.4	0.0380	YES	43.79	-73.79	1.05E+08
North Hudson	108.1	0.0410	YES	43.95	-73.74	9.81E+07
Blue Ridge	87.2	0.0330	YES	43.96	-73.78	1.22E+08
Craig Harbor	86.0	0.0320	YES	44.05	-73.46	1.23E+08
Split Rock Point	88.6	0.0330	YES	44.27	-73.32	1.20E+08
Willsboro Dike (J)	91.8	0.0350	YES	44.45	-73.38	1.16E+08

		Mount Trembleau	83.5	0.0310	YES	44.01	-73.4	1.27E+08
		Poke-O-Moonshine	99.3	0.0370	YES	44.4	-73.52	1.07E+08
Roden-Tice and Wintsch, 2002	CT	1. HB, CT	38.1	0.0144	YES	41.6	-72.92	1.39E+08
		2. HB, CT	34.9	0.0132	YES	41.63	-72.61	1.52E+08
		3. HB, CT	38.2	0.0144	YES	41.79	-72.5	1.39E+08
		4. WCT	31.5	0.0119	YES	41.54	-73.48	1.68E+08
			28.6	0.0108	YES	41.54	-73.48	1.86E+08
		5. WCT	33.8	0.0127	YES	41.56	-73.39	1.57E+08
		6. WCT	37.3	0.0141	YES	41.47	-73.26	1.42E+08
			66.3	0.0250	YES	41.47	-73.26	1.84E+08
		7. WCT	35.0	0.0132	YES	41.46	-73.2	1.52E+08
		8. WCT	35.0	0.0132	YES	41.43	-73.07	1.52E+08
		9. PB, CT	33.7	0.0127	YES	41.46	-73.25	1.57E+08
		10. BH, CT	35.5	0.0134	YES	41.29	-72.56	1.49E+08
			65.4	0.0247	YES	41.29	-72.56	1.86E+08
		11. BH, CT	39.8	0.0150	YES	41.49	-72.57	1.33E+08
			81.5	0.0308	YES	41.49	-72.57	1.50E+08
		12. BH, CT	38.4	0.0145	YES	41.68	-72.42	1.38E+08
		13. BH, CT	46.7	0.0176	YES	41.9	-72.44	1.13E+08
		14. BH, CT	42.0	0.0158	YES	41.76	-72.47	1.26E+08
		15. BH, CT	36.9	0.0139	YES	41.77	-72.46	1.44E+08
		16. BH, CT	37.1	0.0140	YES	41.76	-72.45	1.43E+08
		17. BH, CT	40.5	0.0153	YES	41.85	-72.42	1.31E+08
			83.2	0.0314	YES	41.85	-72.42	1.47E+08
		18. BH, CT	43.2	0.0163	YES	41.84	-72.44	1.23E+08
		19. BH, CT	45.5	0.0172	YES	41.85	-72.46	1.17E+08
		20. M, CT	32.2	0.0122	YES	41.49	-72.44	1.65E+08
		21. M, CT	40.7	0.0154	YES	41.76	-72.4	1.30E+08
		22. CM, CT	40.2	0.0152	YES	41.83	-72.37	1.32E+08
	MA	23. BH, MA	38.1	0.0144	YES	41.43	-72.42	1.39E+08

		24. BH, MA	54.1	0.0204	YES	42.65	-72.47	9.79E+07
		25. BH, MA	53.6	0.0202	YES	42.65	-72.53	9.88E+07
		26. BH, MA	47.7	0.0180	YES	42.67	-72.48	1.11E+08
		27. BH, MA	50.1	0.0189	YES	42.66	-72.47	1.06E+08
			85.2	0.0321	YES	42.66	-72.47	1.43E+08
		28. BH, MA	45.0	0.0170	YES	42.58	-72.38	1.18E+08
		29. BH, MA	50.7	0.0191	YES	42.62	-72.37	1.05E+08
		30. BH, MA	36.4	0.0137	YES	42.38	-72.29	1.46E+08
		31. BH, MA	37.0	0.0139	YES	42.46	-72.26	1.43E+08
			62.1	0.0234	YES	42.46	-72.26	1.96E+08
	NH	32. BH, NH	36.8	0.0139	YES	42.83	-72.36	1.44E+08
Miller and Duddy, 1989	NY	Northern Appalachian Basin	98.1	0.037	YES	42.23	-74.02	1.08E+08
			68.4	0.026	YES	42.23	-74.02	1.55E+08
			64.6	0.024	YES	42.23	-74.02	1.64E+08
			73.1	0.028	YES	42.46	-74.47	1.45E+08
			106.0	0.040	YES	42.46	-74.47	1.00E+08
			80.3	0.030	YES	42.53	-74.89	1.32E+08
			72.6	0.027	YES	42.45	-75.92	1.46E+08
			74.6	0.028	YES	42.9	-76.42	1.42E+08
			42.7	0.016	YES	42.98	-78.71	2.48E+08
			43.1	0.016	YES	42.81	-74.54	2.46E+08
			46.5	0.018	YES	42.99	-76.06	2.28E+08
			71.1	0.027	YES	42.89	-76.61	1.49E+08
			53.0	0.020	YES	42.97	-77.38	2.00E+08
			84.1	0.032	YES	42.19	-74.11	1.26E+08
			69.3	0.026	YES	42.19	-74.11	1.53E+08
			56.4	0.021	YES	42.19	-75.12	1.88E+08
			66.3	0.025	YES	42.38	-75.02	1.60E+08
			66.7	0.025	YES	41.53	-74.7	1.59E+08
			77.9	0.029	YES	41.45	-74.7	1.36E+08

78.5	0.030	YES	41.47	-74.84	1.35E+08
58.6	0.022	YES	41.52	-74.91	1.81E+08
81.5	0.031	YES	41.61	-74.99	1.30E+08
82.8	0.031	YES	41.76	-74.99	1.28E+08
63.1	0.024	YES	41.83	-74.9	1.68E+08
91.4	0.034	YES	41.85	-75.01	1.16E+08
75.7	0.029	YES	41.97	-75.21	1.40E+08
66.3	0.025	YES	42.07	-75.92	1.60E+08
76.3	0.029	YES	42.85	-76.13	1.39E+08
93.0	0.035	YES	42.58	-76.84	1.14E+08
74.6	0.028	YES	42.31	-77.17	1.42E+08
76.8	0.029	YES	42.17	-77.35	1.38E+08
49.8	0.019	NO	42.07	-78.27	2.13E+08
59.2	0.022	YES	42.29	-78.2	1.79E+08
63.9	0.024	YES	42.4	-78.34	1.66E+08
50.2	0.019	YES	42.52	-77.93	2.11E+08
93.0	0.035	YES	41.76	-74.46	1.14E+08
89.1	0.034	YES	41.92	-74.76	1.19E+08
87.6	0.033	YES	42.06	-74.86	1.21E+08
74.1	0.028	YES	42.18	-74.66	1.43E+08
89.8	0.034	YES	42.1	-74.54	1.18E+08
83.5	0.031	YES	41.93	-74.25	1.27E+08
76.8	0.029	YES	41.93	-74.25	1.38E+08
98.1	0.037	YES	41.93	-74.25	1.08E+08
91.4	0.034	YES	42	-74.37	1.16E+08
73.6	0.028	YES	42.62	-74.8	1.44E+08
67.1	0.025	NO	42.15	-78.53	1.58E+08
59.9	0.023	YES	42.1	-77.63	1.77E+08
80.3	0.030	YES	42.1	-76.95	1.32E+08
84.8	0.032	YES	42.08	-76.41	1.25E+08
68.4	0.026	YES	42.85	-76.65	1.55E+08

			72.6	0.027	YES	42.69	-75.38	1.46E+08
			52.0	0.020	YES	42.53	-75.64	2.04E+08
			101.9	0.038	YES	42.51	-76.32	1.04E+08
			80.3	0.030	YES	42.4	-74.18	1.32E+08
			73.1	0.028	YES	41.61	-74.99	1.45E+08
			94.6	0.036	YES	42.7	-73.43	1.12E+08
			163.1	0.062	YES	42.65	-73.51	6.50E+07
Doherty and Lyons, 1980	VT	Mt Monadnock stock	77.4	0.029	YES	44.909	-71.603	1.14E+08
			107.1	0.040	YES	44.909	-71.603	1.65E+08
	NH	Gore Mtn stock	91.9	0.035	YES	44.75	-71.524	9.60E+07
	NH	Ossipee complex	165.2	0.062	YES	43.789	-71.242	1.07E+08
	NH	Belknap stock	98.1	0.037	YES	43.575	-71.398	9.00E+07
	NH	Merrymeeting stock	108.9	0.041	YES	43.497	-71.193	8.10E+07
	NH	Mt Pawtuckaway complex	72.3	0.027	YES	43.128	-71.238	1.22E+08
			163.7	0.062	YES	43.128	-71.238	1.08E+08
	NH	Mad River stock	86.5	0.033	YES	43.948	-71.496	1.02E+08
	VT	Mt Ascutney complex	87.4	0.033	YES	43.427	-72.455	1.01E+08
			141.4	0.053	YES	43.427	-72.455	1.25E+08
	NH	Redstone Quarry White Mtn Batholith	93.9	0.035	YES	44.024	-71.106	9.40E+07
			108.4	0.041	YES	44.024	-71.106	1.63E+08
	NH	Cannon Mtn stock	107.6	0.041	YES	44.168	-71.724	8.20E+07
			102.2	0.039	YES	44.168	-71.724	1.73E+08